

**2019 Fall**

**“Advanced Physical Metallurgy”  
- Non-equilibrium Solidification -**

**10.17.2019**

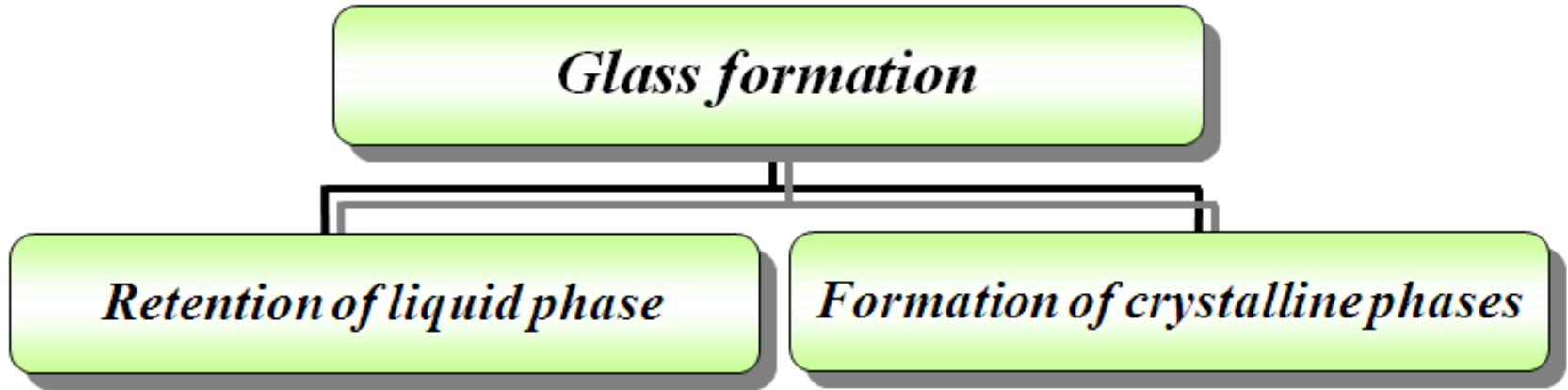
**Eun Soo Park**

**Office: 33-313**

**Telephone: 880-7221**

**Email: [espark@snu.ac.kr](mailto:espark@snu.ac.kr)**

**Office hours: by appointment**



**Glass Formation** results when

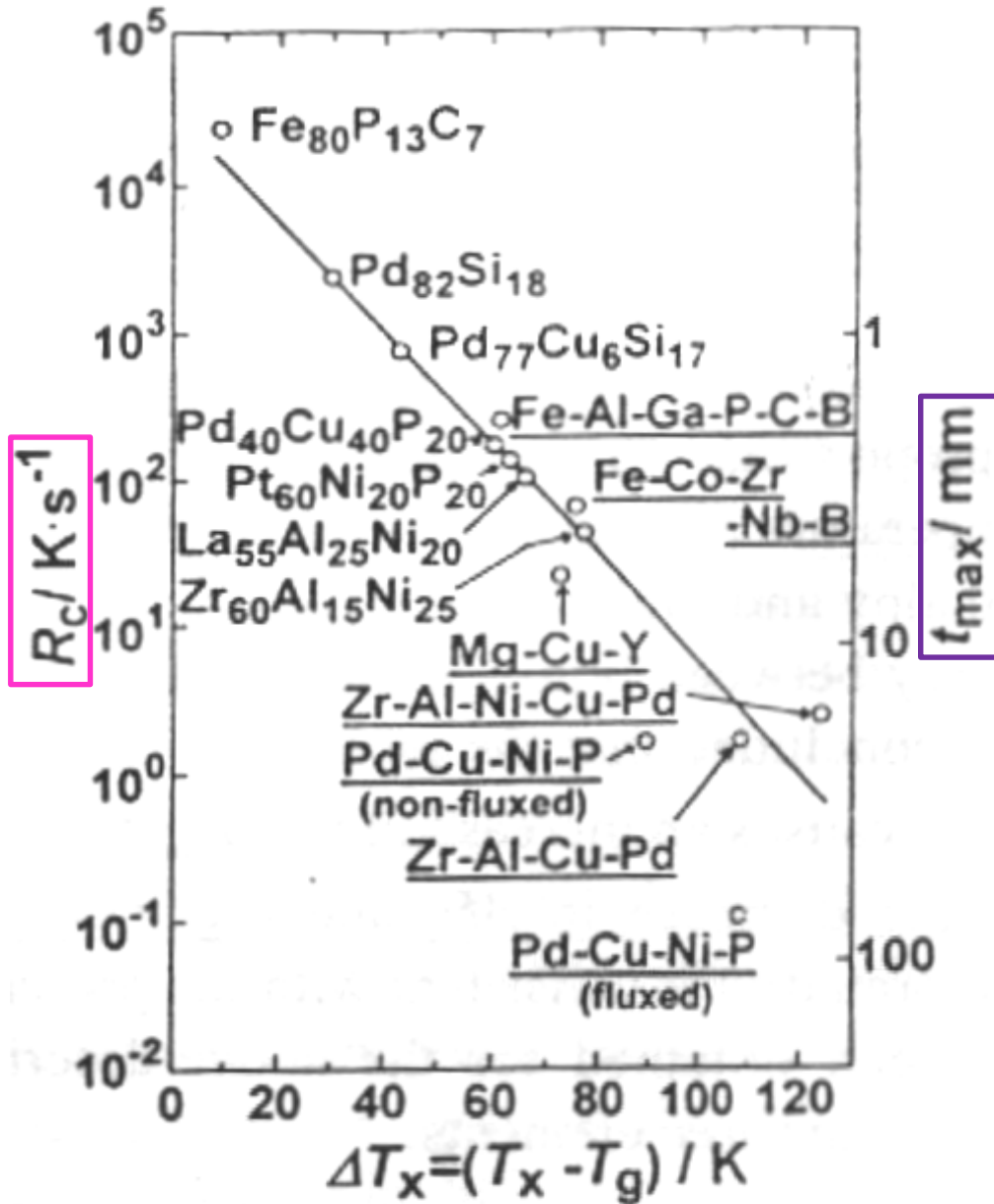
Liquids are cooled to below  $T_m$  ( $T_L$ ) sufficiently fast to avoid crystallization.

- ┌ **Nucleation** of crystalline seeds are avoided
- └ **Growth** of Nuclei into crystallites (crystals) is avoided

Liquid is “**frustrated**” by internal structure that hinders both events

➔ **“Glass Formation”**

Critical cooling rate is inversely proportional to the diameter of ingot.



# Critical Cooling Rates for Various Liquids

**Table 3-5.** Examples of Critical Cooling Rates ( $^{\circ}\text{C}/\text{s}$ ) for Glass Formation

Material	Homogeneous nucleation	Heterogeneous nucleation contact angle (deg)		
		100	60	40
SiO <sub>2</sub> glass <sup>a</sup>	$9 \times 10^{-6}$	$10^{-5}$	$8 \times 10^{-3}$	$2 \times 10^{-1}$
GeO <sub>2</sub> glass <sup>a</sup>	$3 \times 10^{-3}$	$3 \times 10^3$	1	20
Na <sub>2</sub> O·2SiO <sub>2</sub> glass <sup>a</sup>	$6 \times 10^{-3}$	$8 \times 10^{-3}$	10	$3 \times 10^{+2}$
Salol	10			
Water	$10^7$			
Ag	$10^{10}$			
Typical metal <sup>a</sup>	$9 \times 10^8$	$9 \times 10^9$	$10^{10}$	$5 \times 10^{10}$

<sup>a</sup> After P. I. K. Onorato and D. R. Uhlmann, J. Non-Cryst. Sol., 22(2), 367–378 (1976).

## **Q4: Overall Transformation Kinetics–TTT diagram**

**“Johnson-Mehl-Avrami Equation”**

# 5.4 Overall Transformation Kinetics – TTT Diagram

If isothermal transformation,

The fraction of Transformation as a function of Time and Temperature

$$\rightarrow f(t, T)$$

Plot  $f$  vs  $\log t$ .

- isothermal transformation
- $f \sim$  volume fraction of  $\beta$  at any time;  $0 \sim 1$

Plot the fraction of transformation (1%, 99%) in T-log t coordinate.

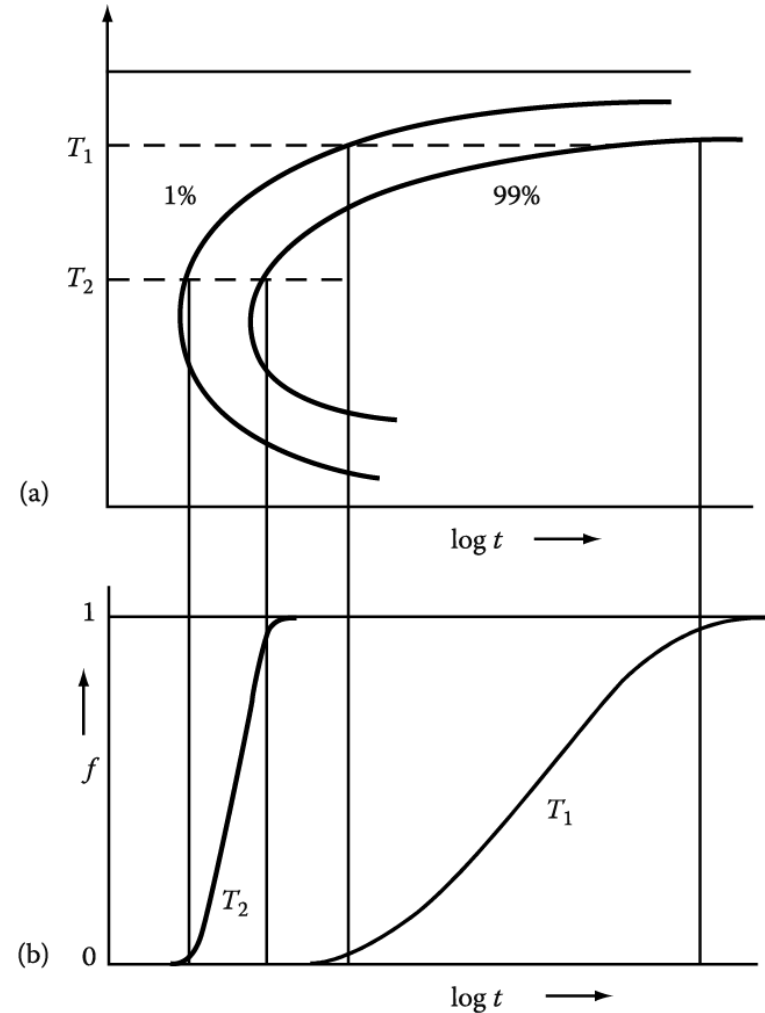


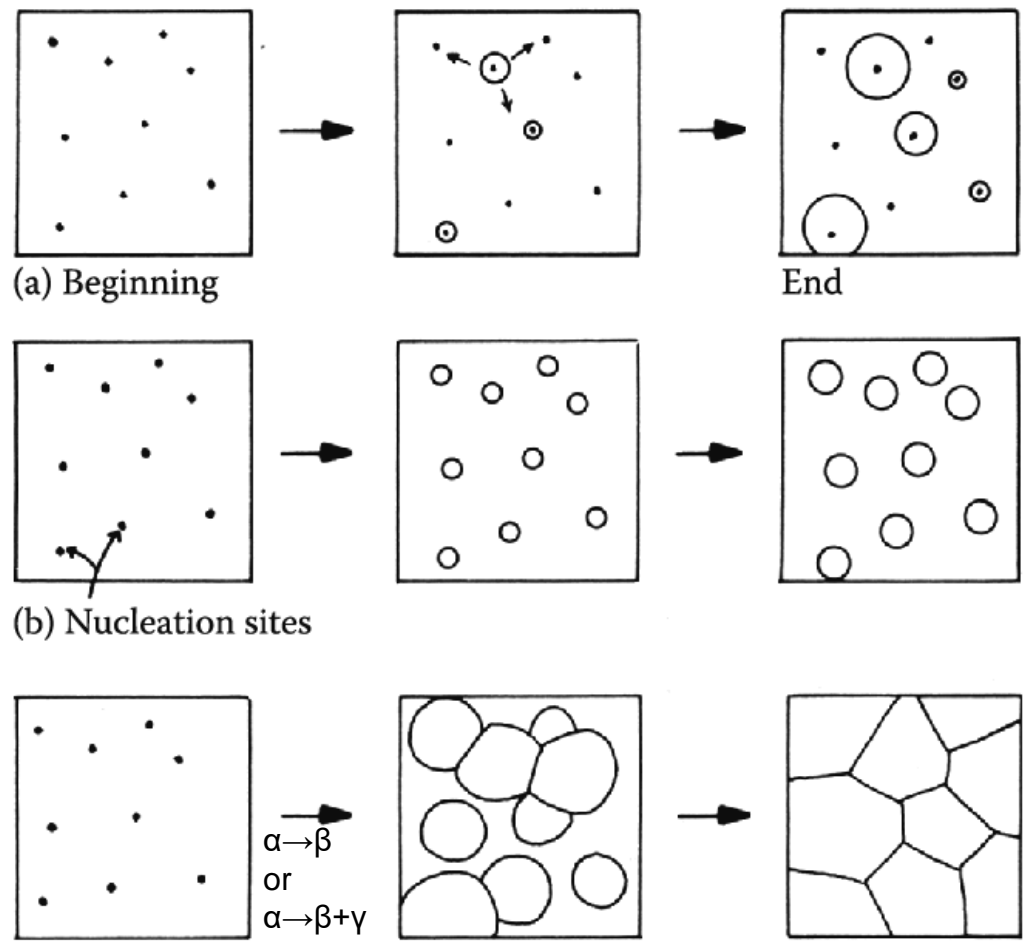
Fig. 5.23 The percentage transformation versus time for different transformation temperatures.

**Influence factors for  $f(t, T)$ : nucleation rate, growth rate, density and distribution of nucleation sites, impingement of adjacent cells**

Example,

**Three Transformation Types**

Wide range of particle sizes



(a) Beginning

End

(b) Nucleation sites

(c) Cellular transformation

**(a) continuous nucleation**

Metastable  $\alpha$  phase with many nucleation sites by quenching to  $T_t$   
 $\rightarrow f$  depends on the *nucleation rate and the growth rate.*

**(b) all nuclei present at  $t = 0$**

$\rightarrow f$  depends on the *number of nucleation sites and the growth rate.*

**(c) All of the parent phase is consumed by the transformation product.**

Transformation terminate by the impingement of adjacent cells growing with a constant velocity.

$\rightarrow$  pearlite, cellular ppt, massive transformation, recrystallization



Fig. 5.24 (a) Nucleation at a constant rate during the whole transformation.  
 (b) Site saturation – all nucleation occurs at the beginning of transformation.  
 (c) A cellular transformation.

# Transformation Kinetics

- Avrami proposed that for a three-dimensional nucleation and growth process kinetic law

$$f = 1 - \exp(-kt^n) \quad \text{Johnson-Mehl-Avrami equation}$$

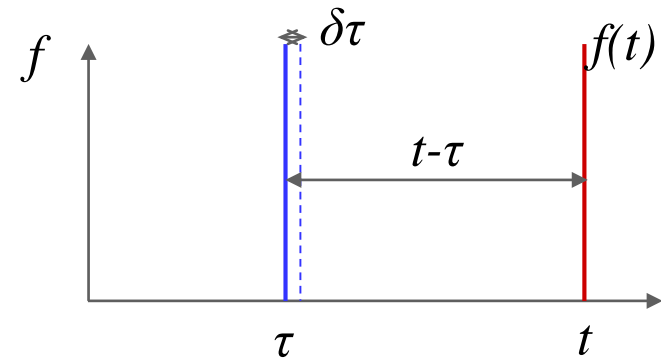
$$f : \text{volume fraction transformed} = \frac{\text{Volume of new phase}}{\text{Volume of specimen}}$$

- Assumption :
  - ✓ reaction produces by nucleation and growth
  - ✓ nucleation occurs randomly throughout specimen
  - ✓ reaction product grows rapidly until impingement



# Constant Nucleation Rate Conditions

- Nucleation rate ( $I$ ) is **constant**.
- Growth rate ( $v$ ) is constant.
- No compositional change



$$df_e = \frac{\left( \begin{array}{l} \text{Vol. of one particle nucleated} \\ \text{during } d\tau \text{ measured at time } t \end{array} \right) \times \left( \begin{array}{l} \text{number of nuclei} \\ \text{formed during } d\tau \end{array} \right)}{\text{Volume of specimen}}$$

$$df_e = \frac{\frac{4}{3} \pi [v(t - \tau)]^3 \times (IV_0 d\tau)}{V_0}$$

$$f_e(t) = \int_0^t I \cdot \frac{4}{3} \pi [v(t - \tau)]^3 d\tau$$

$$= I \cdot \frac{4}{3} \pi v^3 \left[ -\frac{1}{4} (t - \tau)^4 \right]_0^t = \boxed{\frac{1}{3} \pi I v^3 t^4}$$

$$V = \frac{4}{3} \pi r^3 = \frac{4}{3} \pi (vt)^3$$

$$V' = \frac{4}{3} \pi v^3 (t - \tau)^3$$

- do not consider impingement & repeated nucleation

- only true for  $f \ll 1$

As time passes the  $\beta$  cells will eventually impinge on one another and the rate of transformation will decrease again.

# Constant Nucleation Rate Conditions

- consider impingement + repeated nucleation effects

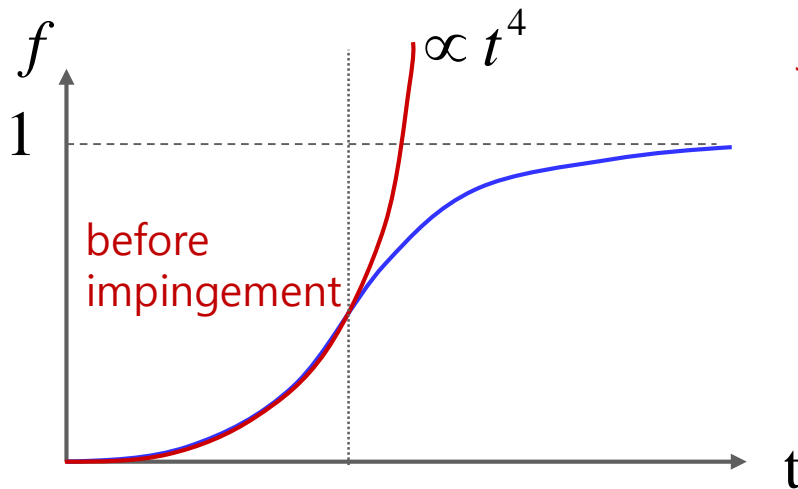
$$df = (1-f)df_e \longrightarrow df_e = \frac{df}{1-f}$$

$$f_e = -\ln(1-f)$$

$$f(t) = 1 - \exp(-f_e(t)) = 1 - \exp\left(-\frac{\pi}{3} I v^3 t^4\right)$$

\* Short time:  
 $1 - \exp(z) \sim z$  ( $z \ll 1$ )

\* Long time:  
 $t \rightarrow \infty, f \rightarrow 1$



Johnson-Mehl-Avrami Equation

$$f = 1 - \exp(-kt^n)$$

$k$ :  $T$  sensitive  $f(I, v)$   $-\frac{\pi}{3} I v^3$   
 $n$ : 1 ~ 4 (depend on nucleation mechanism)

Growth controlled.

Nucleation-controlled.

If no change of nucleation mechanism during phase transformation,  $n$  is not related to  $T$ .

i.e. 50% transform

$$\exp(-0.7) = 0.5$$

$$kt_{0.5}^n = 0.7 \quad t_{0.5} = \frac{0.7}{k^{1/n}} \quad \frac{\pi}{3} I v^3 \quad \Rightarrow \quad t_{0.5} = \frac{0.9}{N^{1/4} v^{3/4}}$$

Rapid transformations are associated with (large values of  $k$ ), or (rapid nucleation and growth rates)

## 2.5.2 Kinetics of Glass Formation

### A. Homogeneous Nucleation rate, $I$ (by David Turnbull)

$$I = \frac{k_n}{\eta(T)} \exp\left[-\frac{b\alpha^3\beta}{T_r(\Delta T_r)^2}\right] \quad (2.4)$$

where

$b$  is a shape factor ( $= 16\pi/3$  for a spherical nucleus)

$k_n$  is a kinetic constant

$\eta(T)$  is the shear viscosity of the liquid at temperature  $T$

$T_r$  is the reduced temperature ( $T_r = T/T_l$ )

$\Delta T_r$  is the reduced supercooling ( $\Delta T_r = 1 - T_r$ )

$\alpha$  and  $\beta$  are dimensionless parameters related, respectively, to the liquid/solid interfacial energy ( $\sigma$ ) and to the molar entropy of fusion,  $\Delta S_f$

Thus,

$$\alpha = \frac{\left(N_A \bar{V}^2\right)^{1/3} \sigma}{\Delta H_f}$$

$$\beta = \frac{\Delta S_f}{R}$$

where

$N_A$  is Avogadro's number

$\bar{V}$  is the molar volume of the crystal

$R$  is the universal gas constant

## A. Homogeneous Nucleation rate, $I$ (by David Turnbull)

$$I = \frac{k_n}{\eta(T)} \exp\left[-\frac{b\alpha^3\beta}{T_r(\Delta T_r)^2}\right]$$

$$\alpha = \frac{\left(N_A \bar{V}^2\right)^{1/3} \sigma}{\Delta H_f}$$

$$\beta = \frac{\Delta S_f}{R}$$

1)  $\eta \uparrow$  (dense random packed structure)  $\rightarrow I \downarrow$

2) For given  $T$  and  $\eta$ ,  $\alpha^3\beta \uparrow$  ( $\sigma$  solid interfacial E &  $\Delta S_f \uparrow / \Delta H_f \downarrow$ )  $\rightarrow I \downarrow$

3)  $\eta \sim T_{rg}$  ( $=T_g/T_l$ ) &  $\alpha^3\beta \sim$  thermal stability of supercooled liquid

\* For metallic melt :  $\alpha\beta^{1/3} \sim 0.5$

\* if  $\alpha\beta^{1/3} > 0.9$ , impossible to crystallization by homogeneous nucleation  
under any cooling condition

\* if  $\alpha\beta^{1/3} \leq 0.25$ , difficult to prevent crystallization

## B. Growth rate of a crystal from an undercooled liquid, $U$

$$U = \frac{10^2 f}{\eta} \left[ 1 - \exp\left(-\frac{\Delta T_r \Delta H_f}{RT}\right) \right] \quad (2.7)$$

where  $f$  represents the fraction of sites at the crystal surfaces where atomic attachment can occur (=1 for close-packed crystals and  $0.2 \Delta T_r$  for faceted crystals). Here also we can see that  $U$  decreases as  $\eta$  increases, and will thus contribute to increased glass formability.

- 1)  $\eta \uparrow$  (dense random packed structure)  $\rightarrow U \downarrow$
  - 2) For given  $T, I$  &  $U \sim \eta \rightarrow T_{rg}$  or  $\alpha, \beta \uparrow \rightarrow \text{GFA} \uparrow$
  - 3)  $f \downarrow$  through atomic rearrangement like local ordering or segregation  $\rightarrow U \downarrow$
- \* metallic melt:  $\alpha\beta^{1/3} \sim 0.5 / T_{rg} > 2/3 \sim \text{high GFA}$
- \* Pure metal:  $R_c \sim 10^{10-12}$  K/s, but if  $T_{rg} = 0.5$ ,  $R_c \sim 10^6$  K/s

Based on the treatment of Uhlmann [25], Davies [26] combined the values of  $I$  and  $U$  (calculated using Equations 2.4 and 2.7, respectively) with the Johnson–Mehl–Avrami treatment of transformation kinetics, and calculated the fraction of transformed phase  $x$  in time  $t$ , for small  $x$ , as

$$C. \quad x = \frac{1}{3} \pi I U^3 t^4 \quad (2.8)$$

Substituting the values of  $I$  and  $U$  in Equation 2.8, the time needed to achieve a small fraction of crystals from the melt was calculated as

$$t \approx \frac{9.3 \eta a_o^2 x}{k T f^3 \bar{N}_v} \left[ \frac{\exp\left(\frac{1.07}{\Delta T_r^2 T_r^3}\right)}{\left\{1 - \exp\left(-\frac{\Delta H_f \Delta T_r}{RT}\right)\right\}^3} \right]^{1/4} \quad (2.9)$$

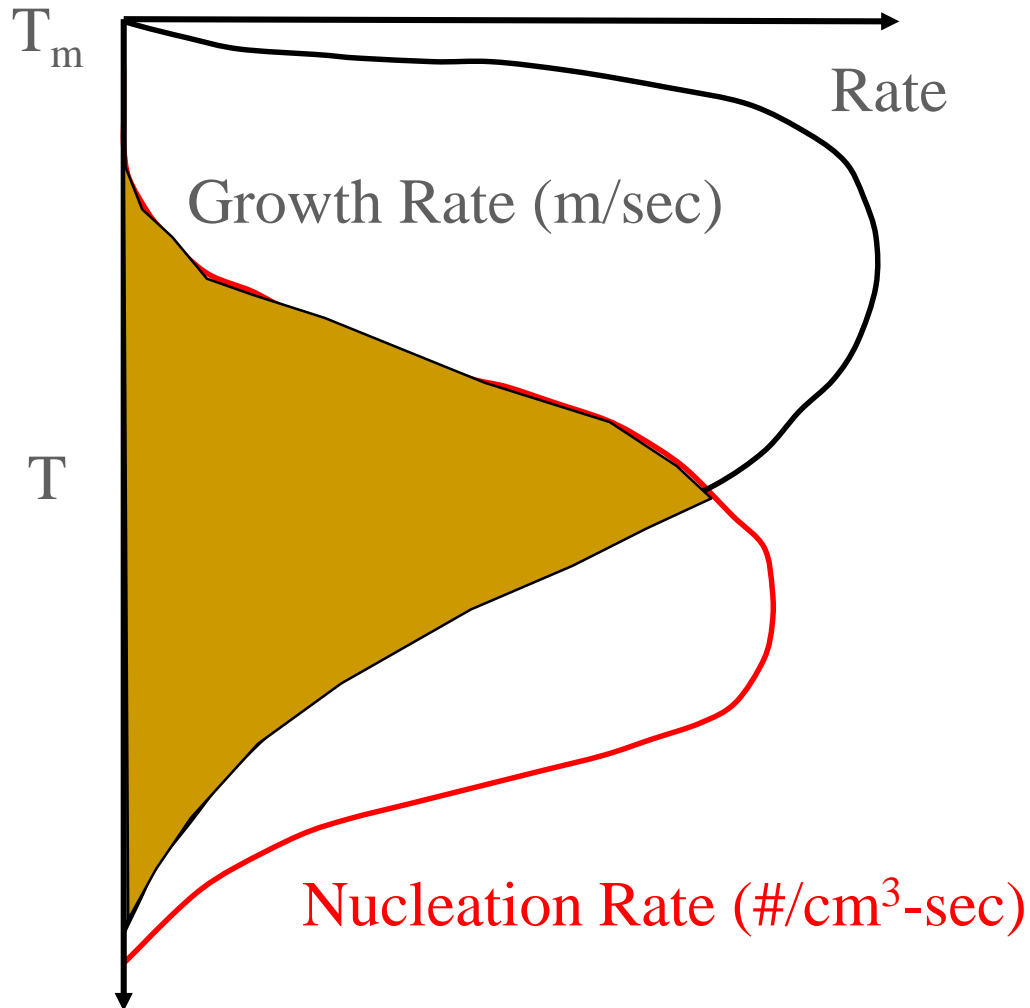
where

$a_o$  is the mean atomic diameter

$\bar{N}_v$  is the average volume concentration of atoms, and all the other parameters have the same meaning, as described earlier

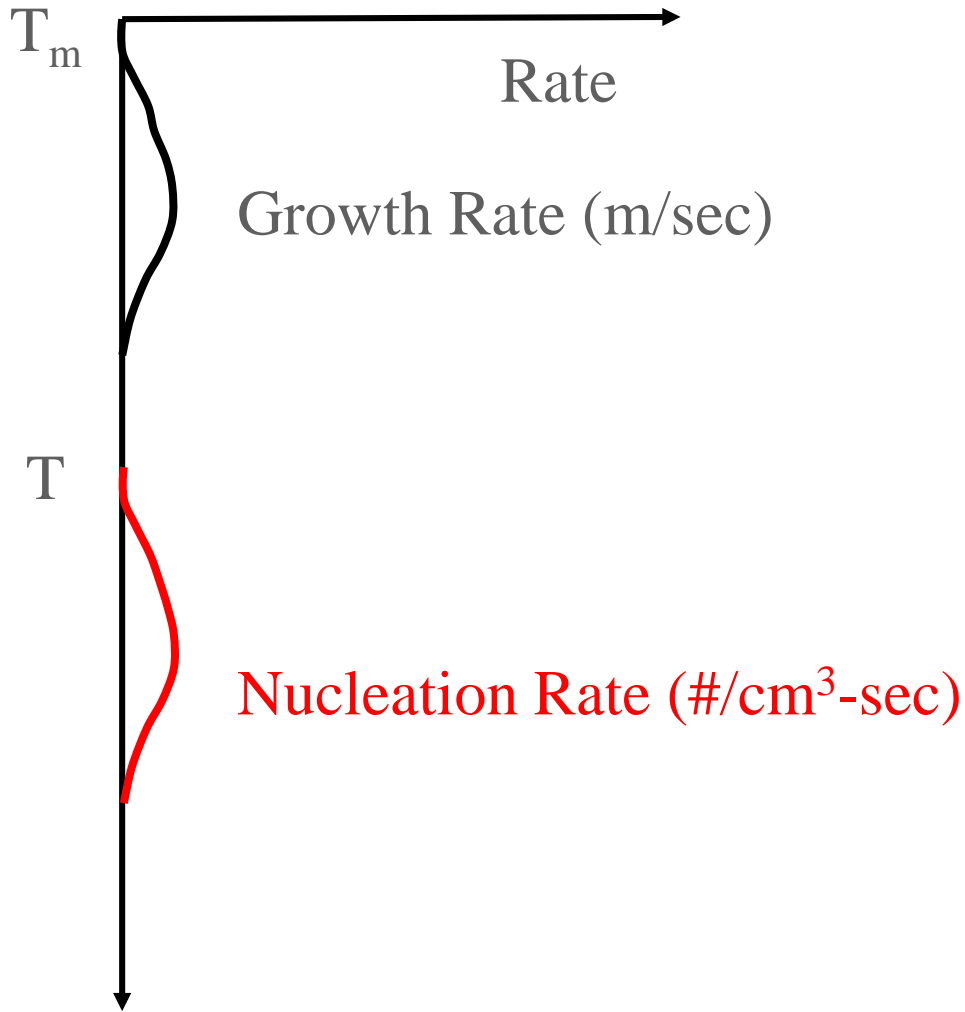
A time–temperature–transformation ( $T$ – $T$ – $T$ ) curve was then computed by calculating the time,  $t$ , as a function of  $T_v$  to transform to a barely detectable fraction of crystal, which was arbitrarily taken to be  $x = 10^{-6}$ .

# Nucleation and Growth Rates – Poor Glass Formers



- Strong overlap of growth and nucleation rates
- Nucleation rate is high
- Growth rate is high
- Both are high at the same temperature

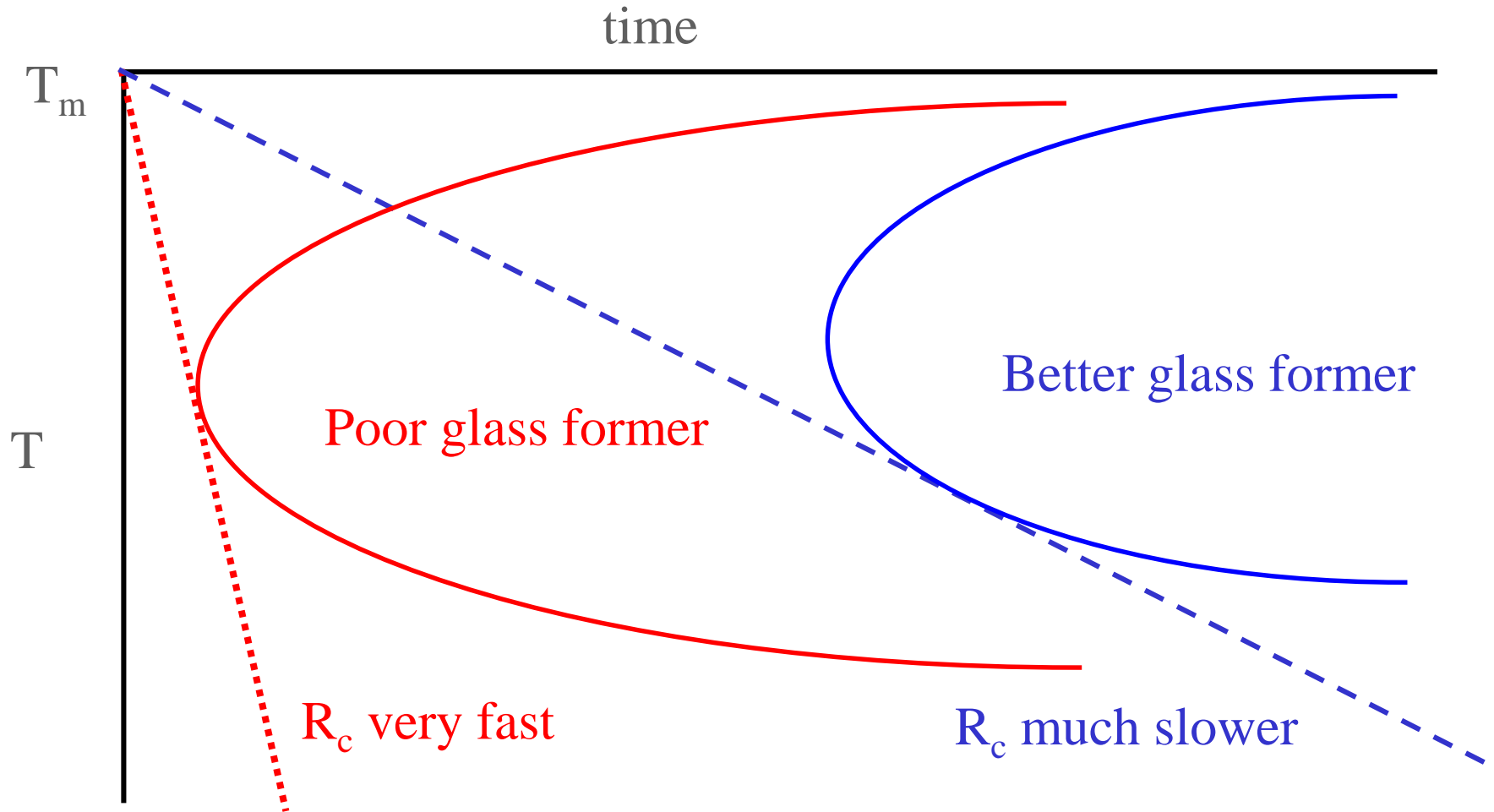
# Nucleation and Growth Rates – Good Glass Formers



- No overlap of growth and nucleation rates
- Nucleation rate is small
- Growth rate is small
- At any one temperature one of the two is zero



# TTT curves and the critical cooling rate, $R_c$



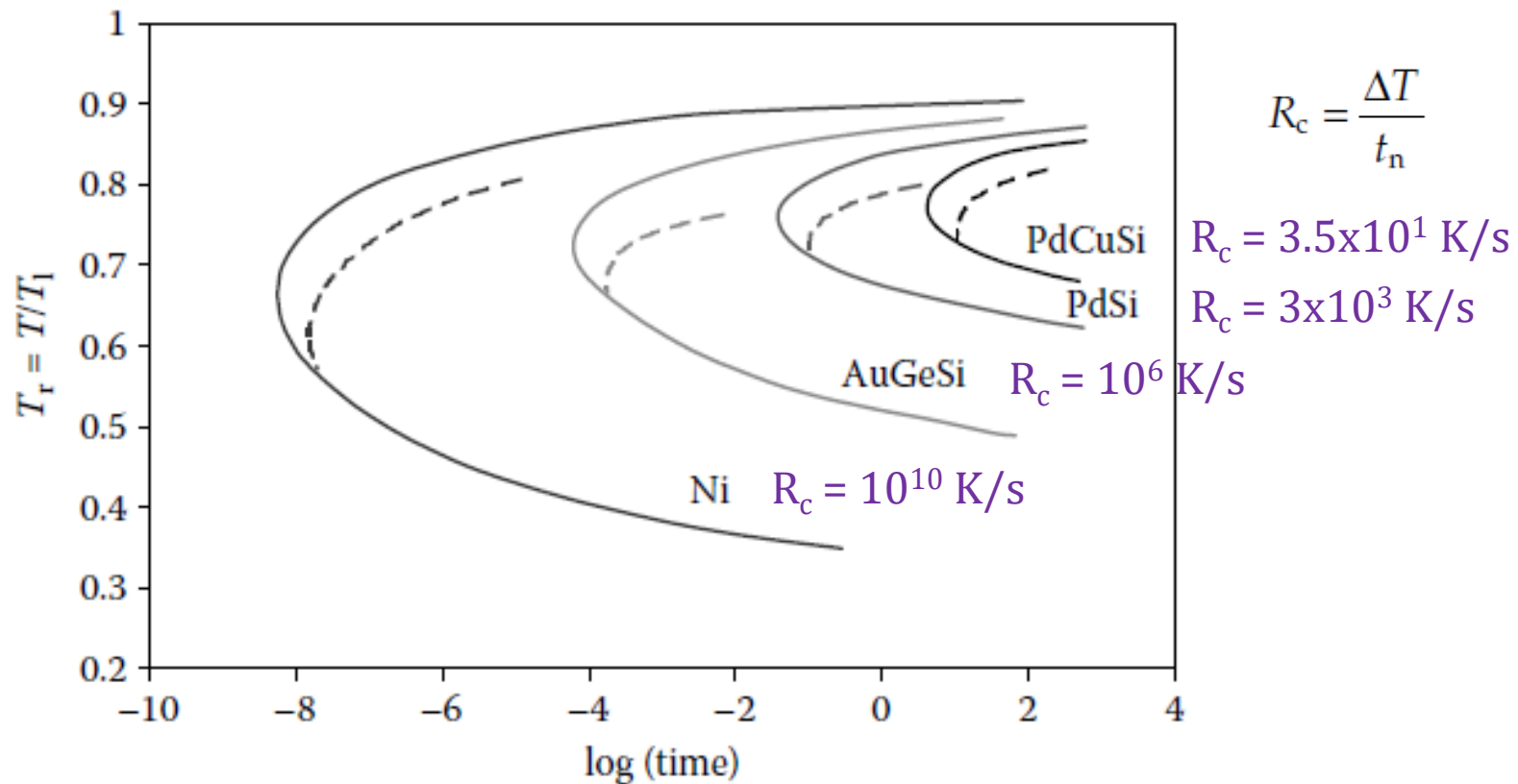


**FIGURE 2.3**

Time-temperature-transformation ( $T$ - $T$ - $T$ ) curves (solid lines) and the corresponding continuous cooling transformation curves (dashed lines) for the formation of a small volume fraction for pure metal Ni, and  $\text{Au}_{78}\text{Ge}_{14}\text{Si}_8$ ,  $\text{Pd}_{82}\text{Si}_{18}$ , and  $\text{Pd}_{78}\text{Cu}_6\text{Si}_{16}$  alloys.

$T_{rg}$

1/4

1/2

2/3

# \* Time-Temperature-Transformation diagrams

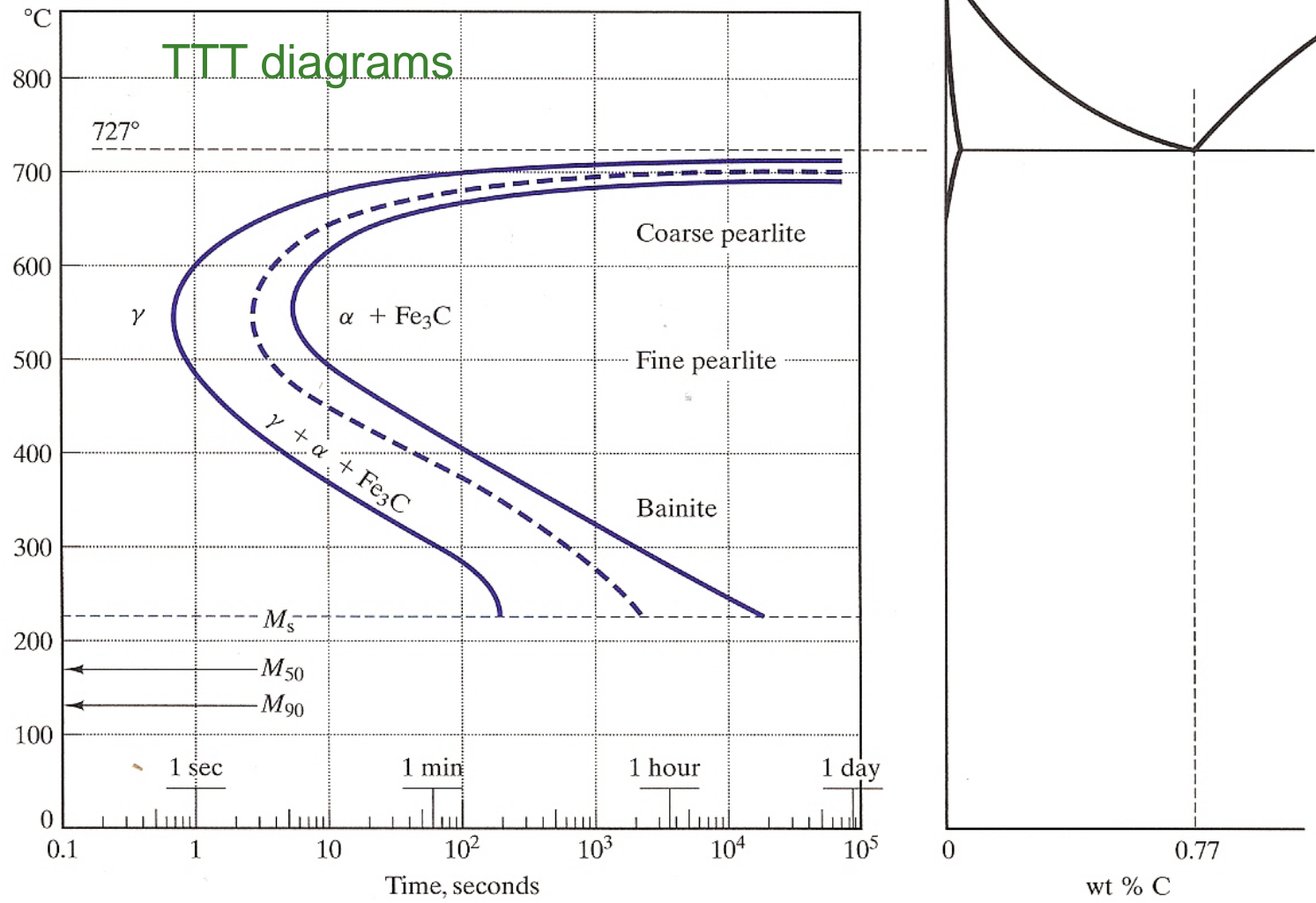


**FIGURE 10.11** A more complete TTT diagram for eutectoid steel than was given in Figure 10.7. The various stages of the time-independent (or diffusionless) martensitic transformation are shown as horizontal lines.  $M_s$  represents the start,  $M_{50}$  represents 50% transformation, and  $M_{90}$  represents 90% transformation. One hundred percent transformation to martensite is not complete until a final temperature ( $M_f$ ) of  $-46^\circ\text{C}$ .

# \* Continuous Cooling Transformation diagrams

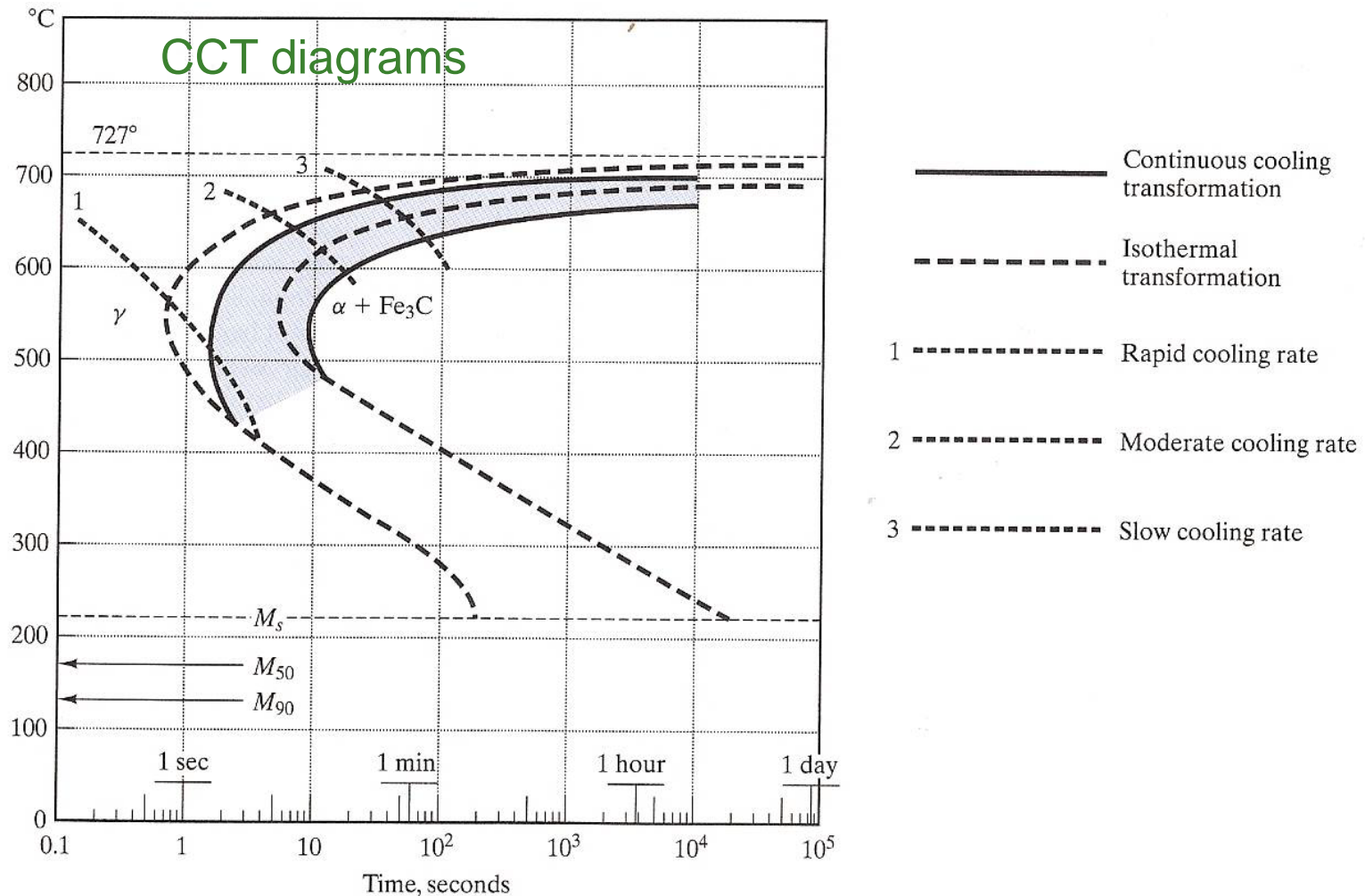
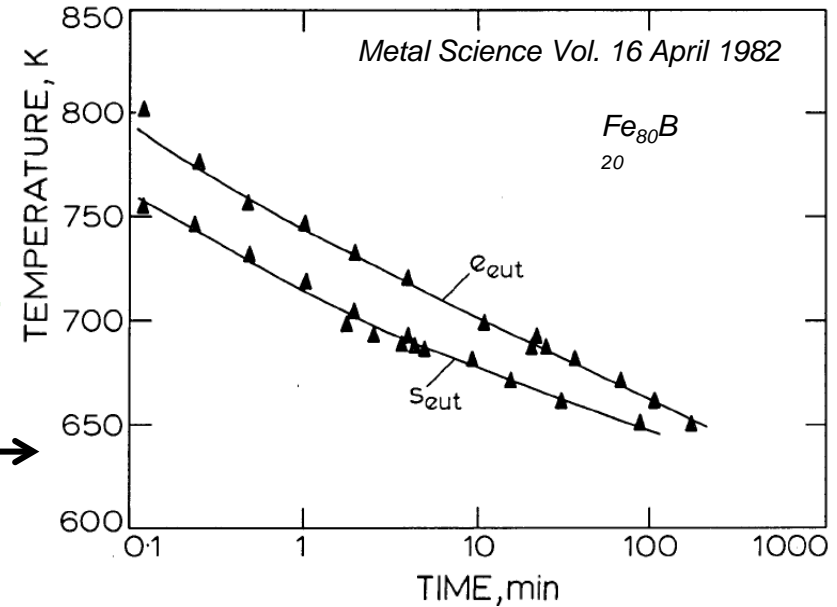
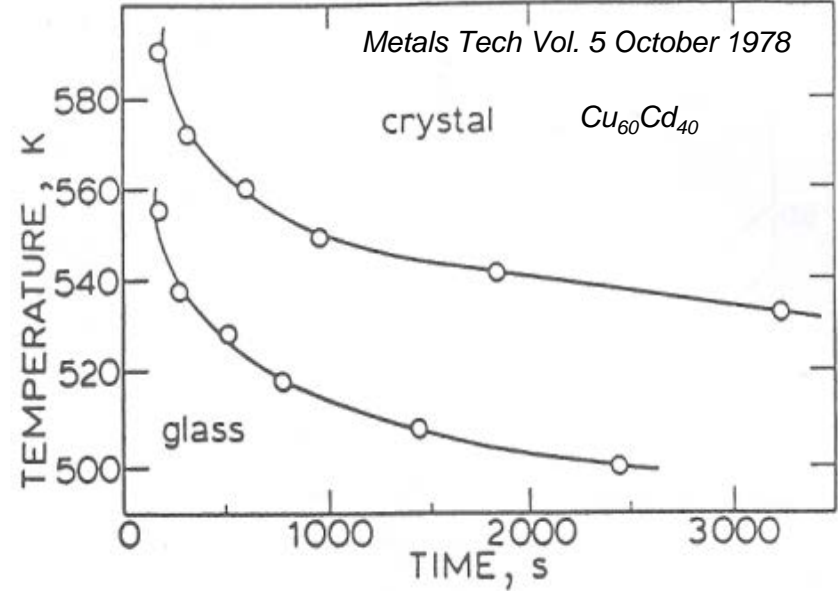
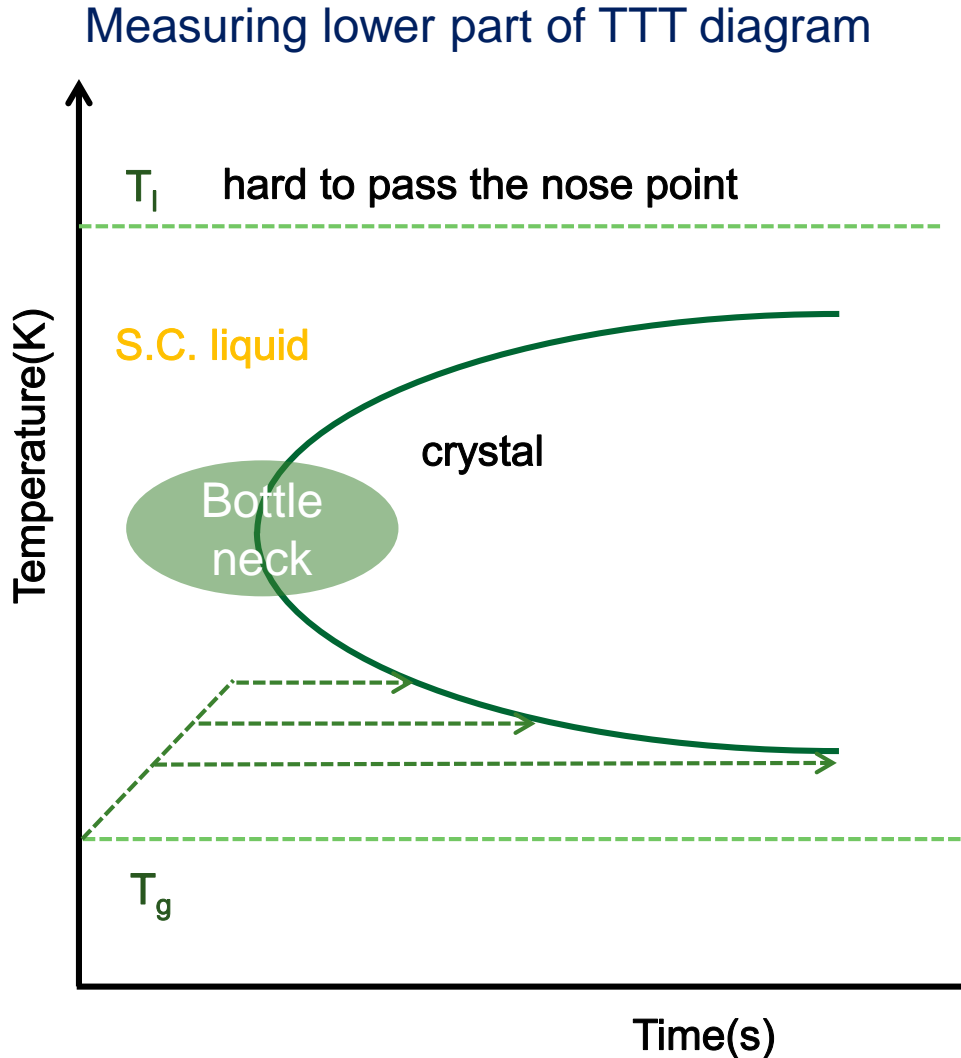


**FIGURE 10.14** A continuous cooling transformation (CCT) diagram is shown superimposed on the isothermal transformation diagram of Figure 10.11. The general effect of continuous cooling is to shift the transformation curves downward and toward the right. (After Atlas of Isothermal Transformation and Cooling Transformation Diagrams, American Society for Metals, Metals Park, OH, 1977.)

## **Q5: Measurement of TTT diagram**

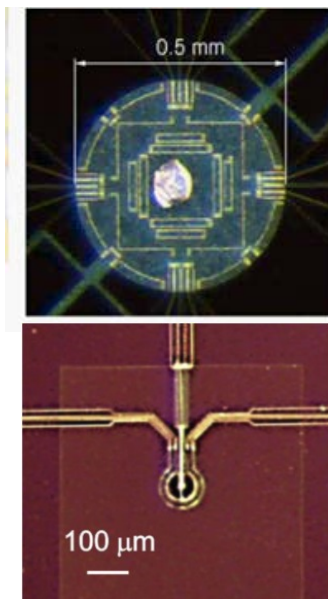
# Measurement of TTT Diagram during Heating by DSC/DTA



## Study of hidden kinetics via fast heating



- Heating rate :  $4 \cdot 10^4$  K/s
- Cooling rate :  $4 \cdot 10^3$  K/s
- Temperature range:  $-90^\circ\text{C} - 1000^\circ\text{C}$



UFS

$-90 - 450^\circ\text{C}$

Limited heating rate  $\sim 3 \cdot 10^4$  K/s

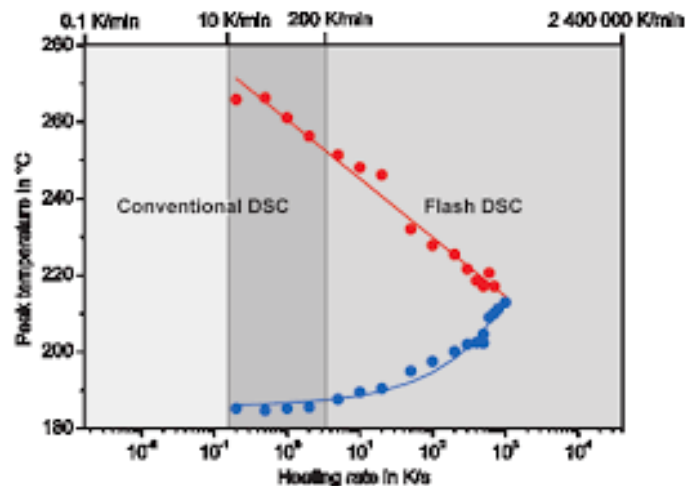
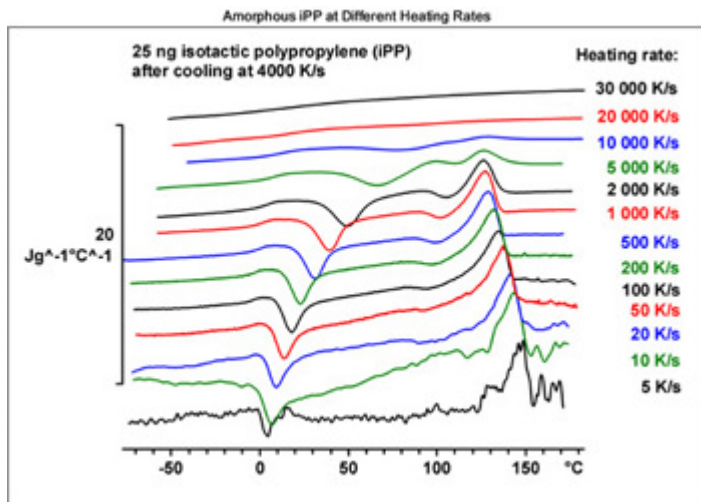
Stable data regardless of sample weight

UFH

$-90 - 1000^\circ\text{C}$

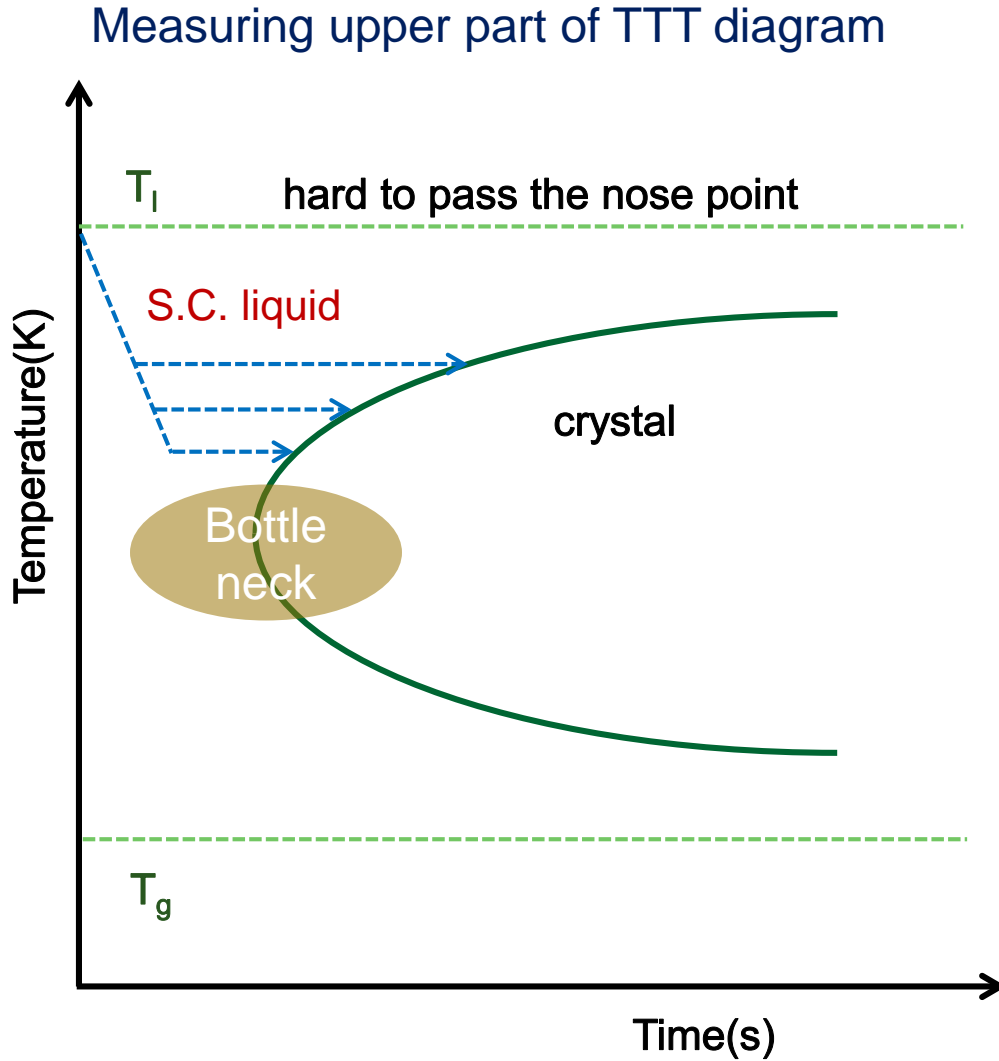
Sample weight less than 100ng is recommended

Extreme experimental condition  $\rightarrow$  hidden kinetics of materials

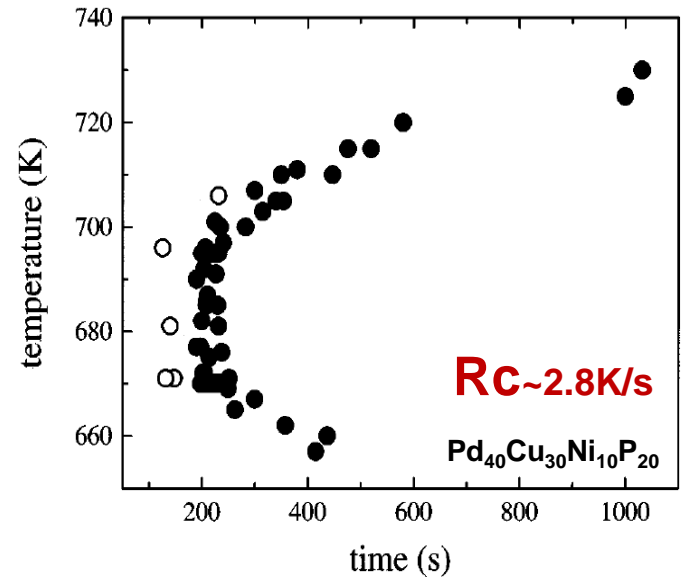
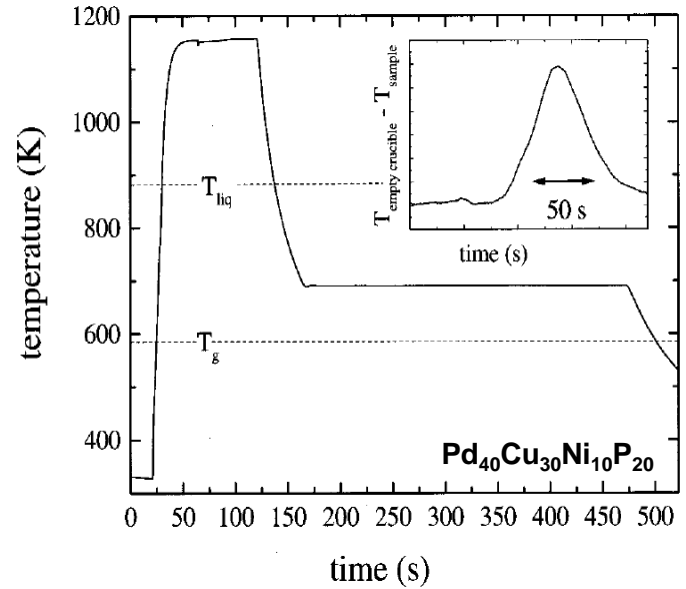




# Measurement of TTT Diagram during Heating by DSC/DTA



*Appl. Phys. Lett.*, vol. 77, No. 8, 32 August 2000





# Calculation of Time-Temperature-Transformation Diagram

## Nucleation Rate

$$I = n v \exp(-N W^* / RT) \exp(-\Delta E_D / RT)$$

$W^*$ : thermodynamic energy barrier to form nuclei

$$W^* = 16 \pi \sigma^3 / 3 (\Delta G_{\text{cryst}}(T))^2$$

$$I = n v \exp(-16 \pi \sigma^3 / 3 (\Delta G_{\text{cryst}}(T))^2 / RT) \exp(-\Delta E_D / RT)$$

## Growth rate

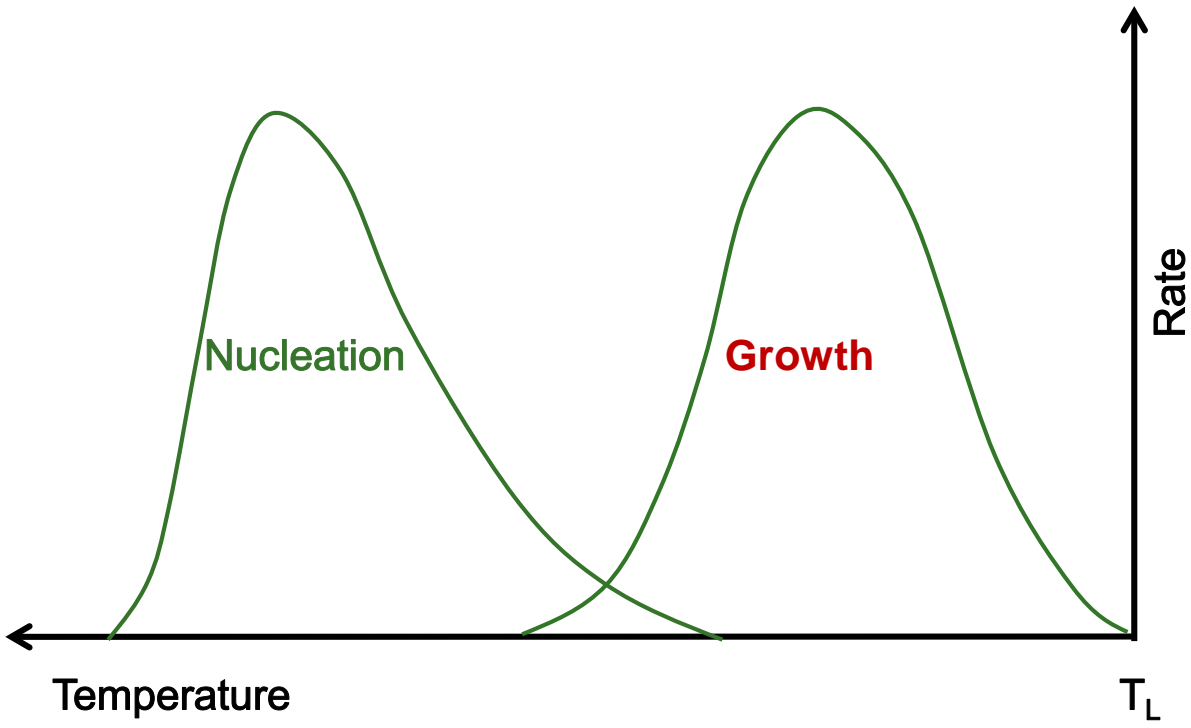
$$\mu = a v \exp(-\Delta E_D / RT) \times (1 - \exp(\Delta G_{\text{cryst}} / RT))$$

$D$ : diffusion coefficient       $E_D$ : diffusion energy barrier to form nuclei

$$D(T) = a^2 v \exp(-\Delta E_D / RT) = f RT / 3 N \pi a^2 \eta(T)$$

Stokes-Einstein relation between  $D$  and  $\eta$

$$\mu(T) = (f RT / 3 N \pi a^2 \eta(T)) (1 - \exp(\Delta G_{\text{cryst}} / RT))$$



# Calculation of Time-Temperature-Transformation Diagram

## Nucleation Rate

$$I = n v \exp(-NW^*/RT) \exp(-\Delta E_D/RT)$$

$W^*$ : thermodynamic energy barrier to form nuclei

$$W^* = 16\pi\sigma^3/3(\Delta G_{\text{cryst}}(T))^2$$

$$I = n v \exp(-16\pi\sigma^3/3(\Delta G_{\text{cryst}}(T))^2/RT) \exp(-\Delta E_D/RT)$$

## Growth rate

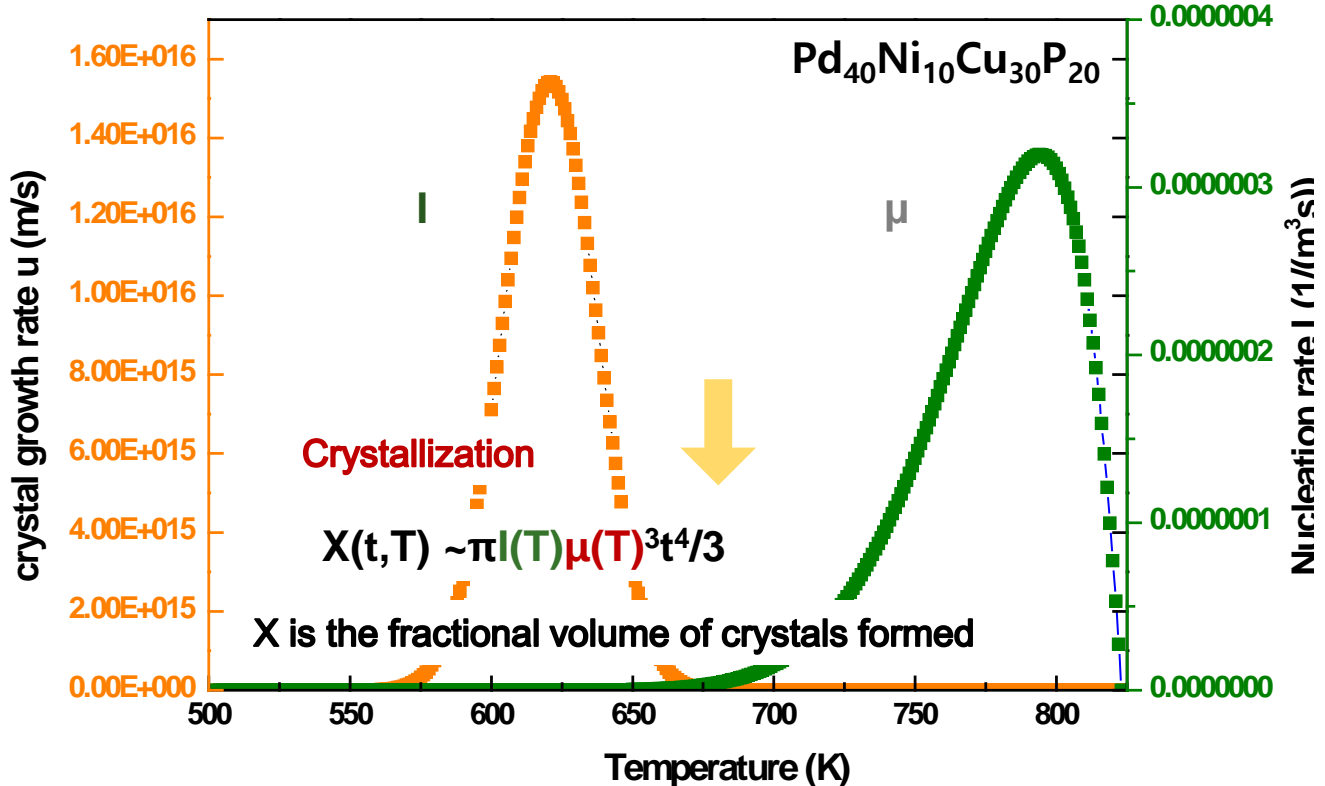
$$\mu = a v \exp(-\Delta E_D/RT) \times (1 - \exp(\Delta G_{\text{cryst}}/RT))$$

$D$ : diffusion coefficient       $E_D$ : diffusion energy barrier to form nuclei

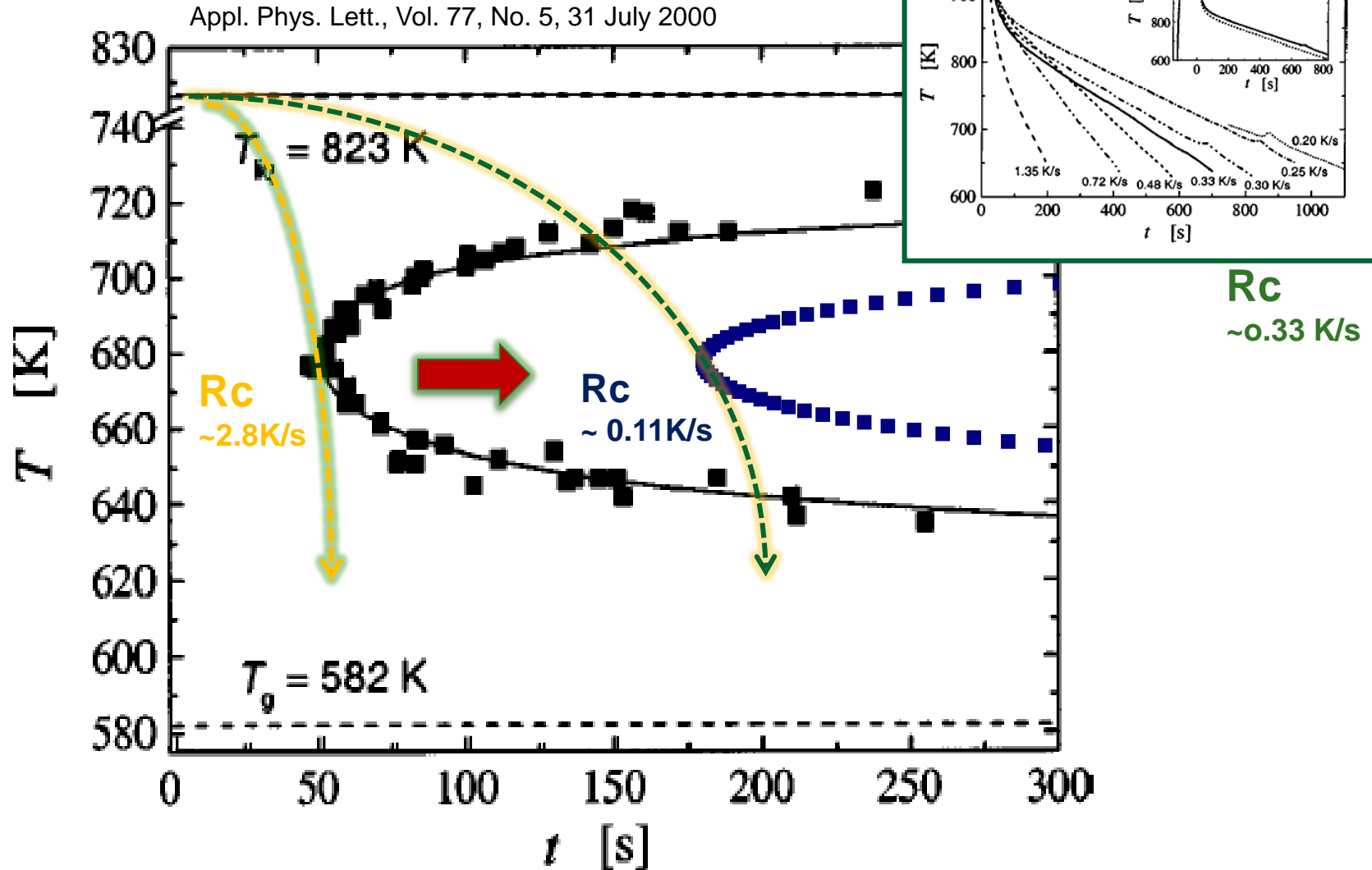
$$D(T) = a^2 v \exp(-\Delta E_D/RT) = fRT/3N\pi a^2 \eta(T)$$

Stokes-Einstein relation between  $D$  and  $\eta$

$$\mu(T) = (fRT/3N\pi a^2 \eta(T)) (1 - \exp(\Delta G_{\text{cryst}}/RT))$$

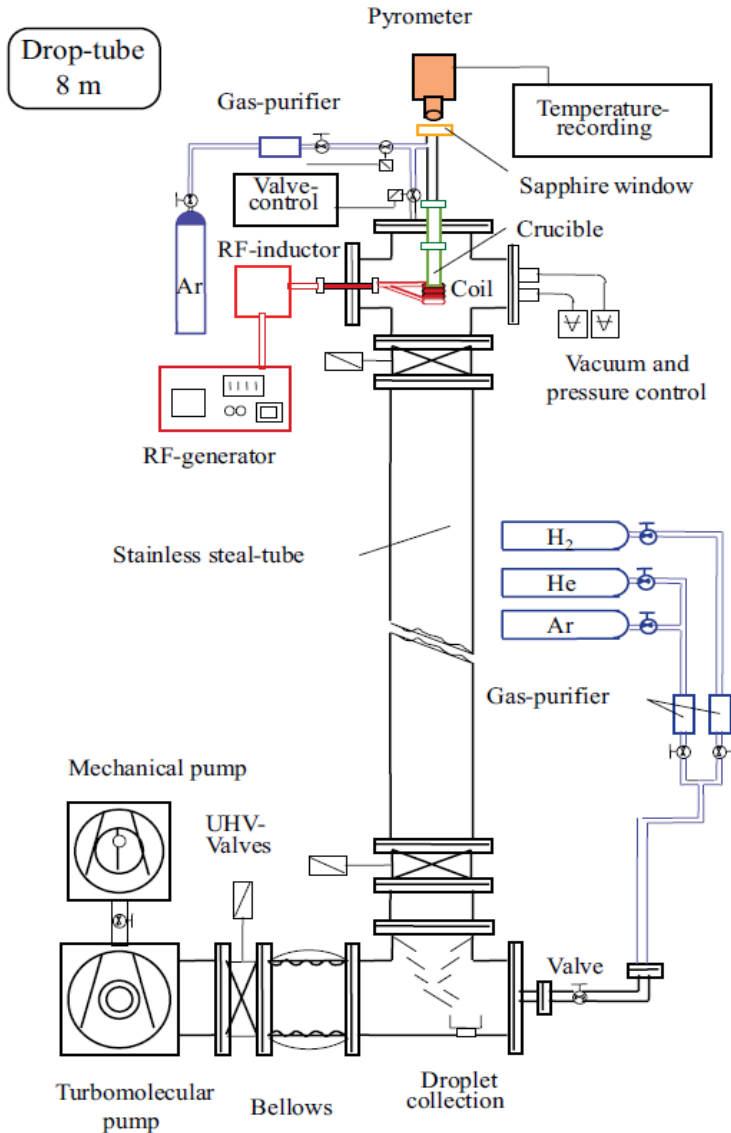


# TTT Diagrams of Pd<sub>40</sub>Cu<sub>30</sub>Ni<sub>10</sub>P<sub>20</sub>



# Measurement of TTT Diagram by Drop Tube Technique

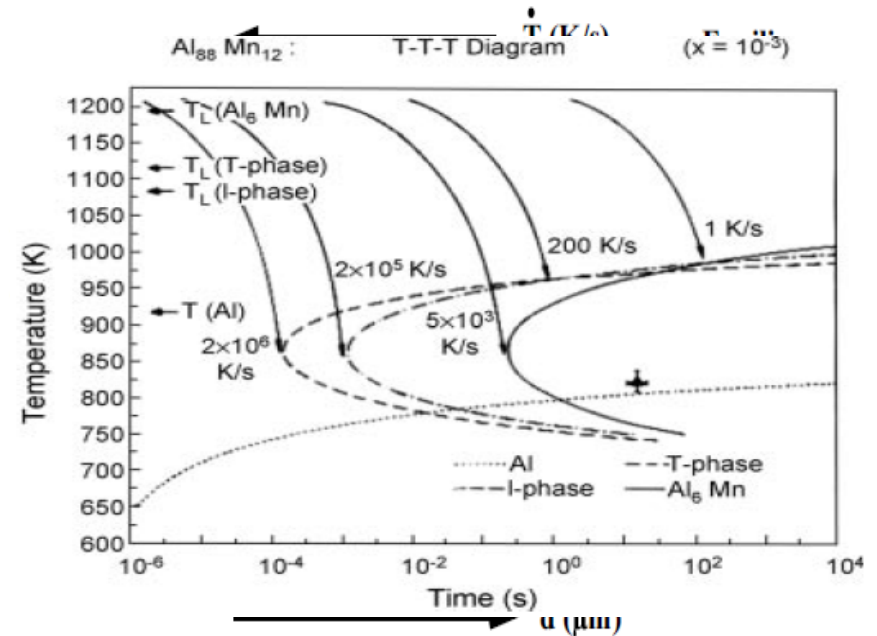
*Solidification of containerless undercooled Melts, edited by Dieter M. Herlach and Douglas M. Matson, 2012, p.1-7*



► Schematic view of DLR drop tube

## Drop tube technique

- rapid cooling of small particles by dispersion of the melt
- reduction of heterogeneous nucleation by containerless processing



- TTT diagram of the droplets of  $\text{Al}_{88}\text{Mn}_{12}$  alloy in the solidification of droplet droplets of  $\text{Al}_{88}\text{Mn}_{12}$

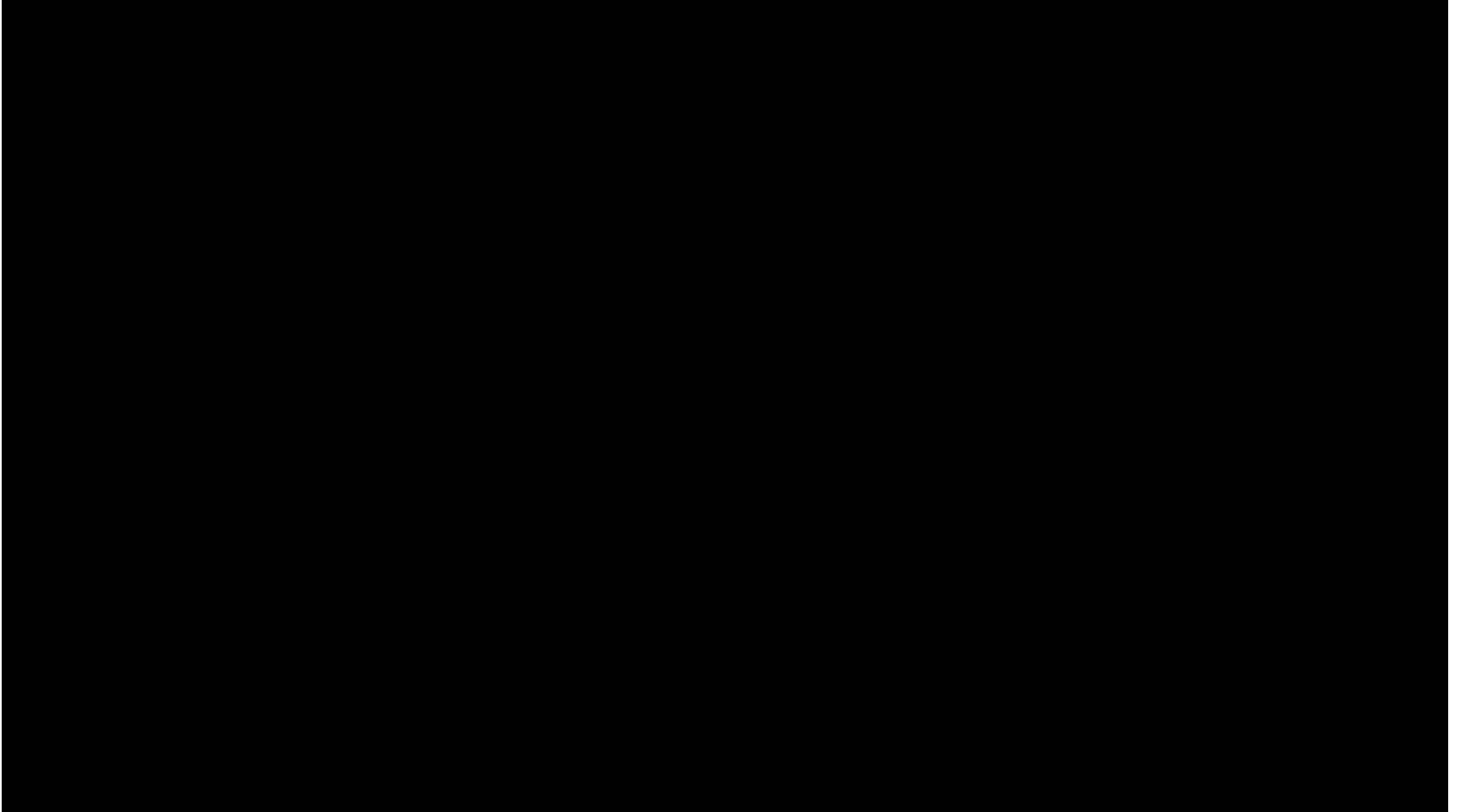
# Electrostatic Levitation in KRISS



한국표준과학연구원

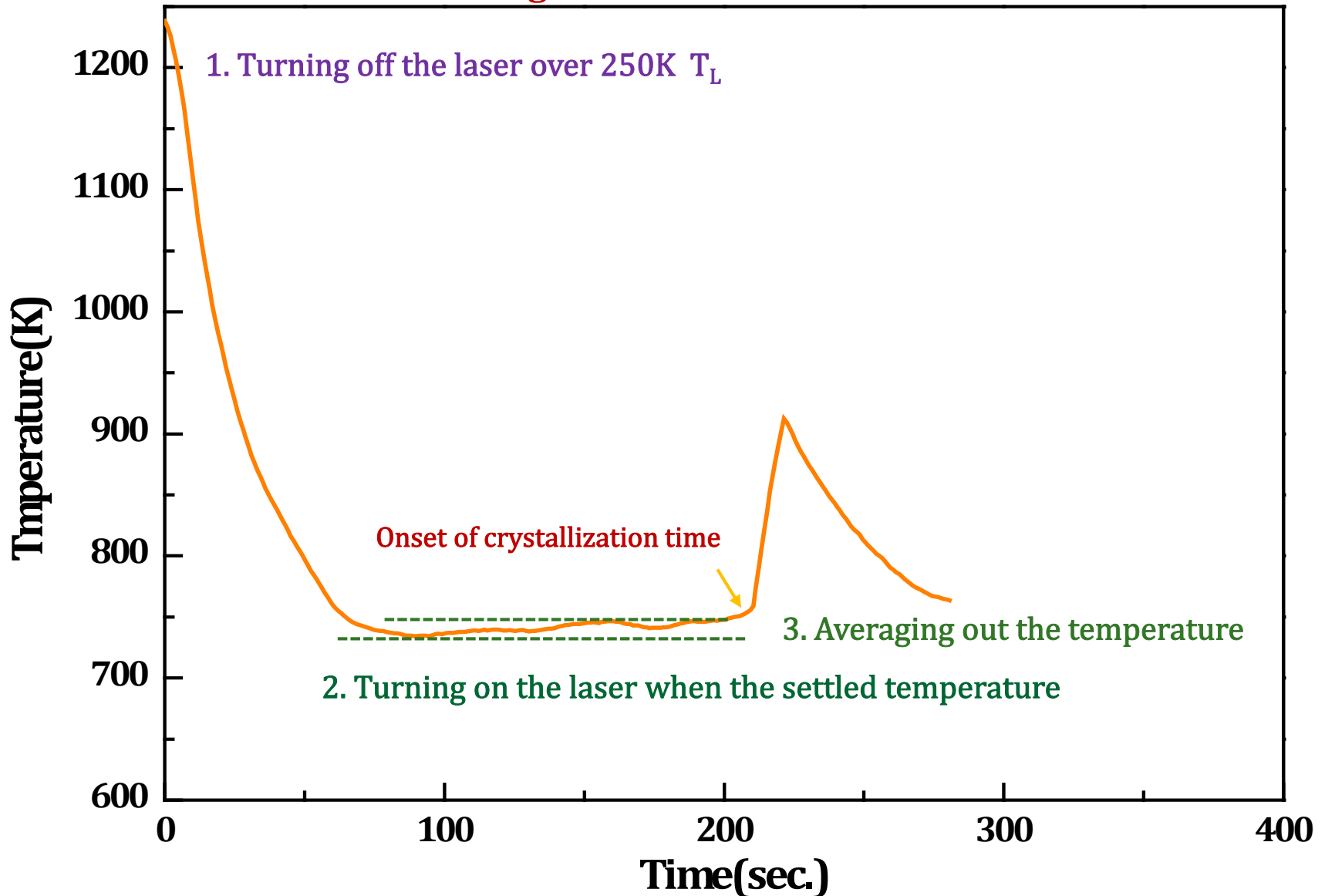
공중부양 초고온 물성 측정 기술 개발

# Electrostatic Levitation in KRISS

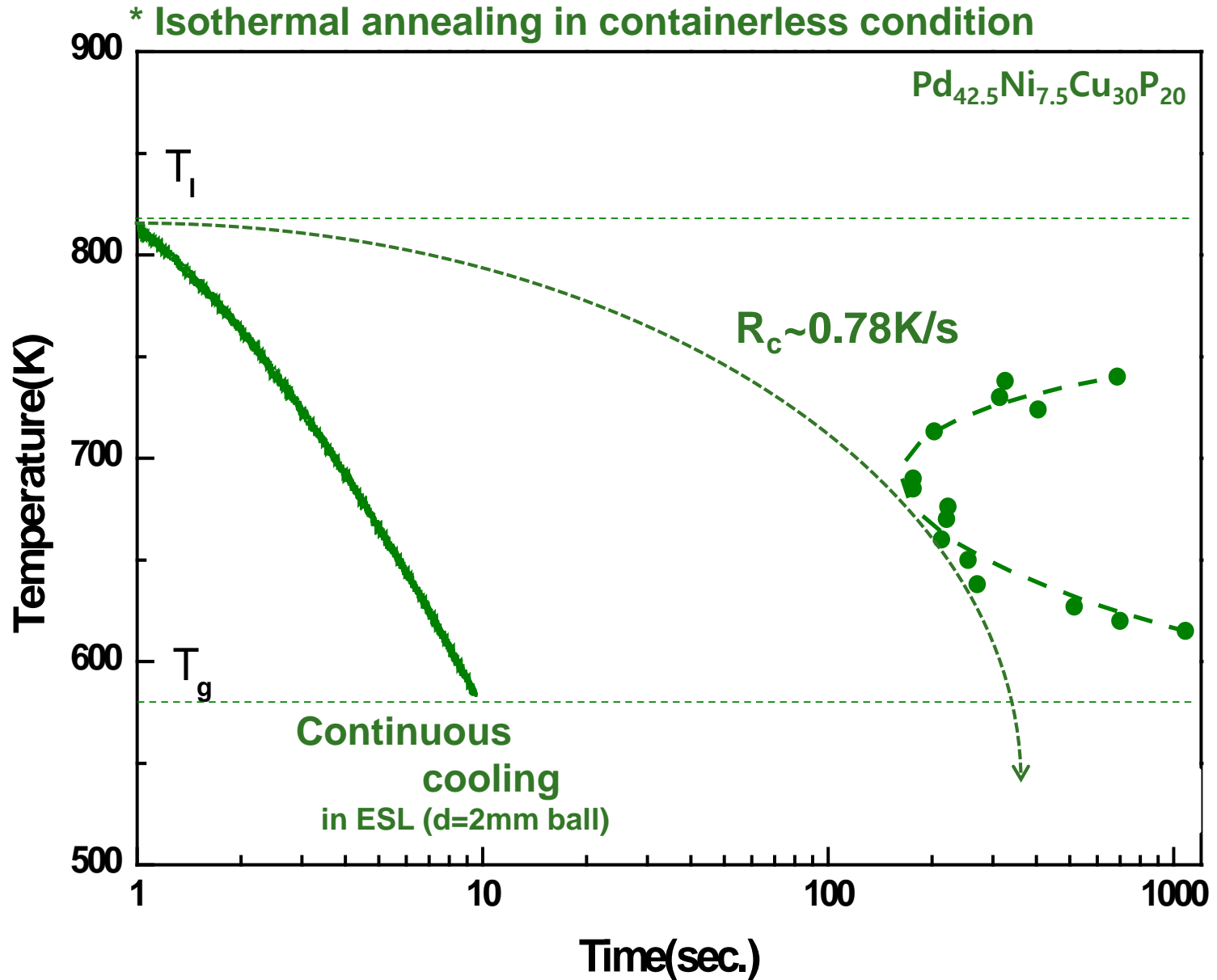


# Measurement of TTT Diagram by ESL Technique

**\* Isothermal annealing in containerless condition**

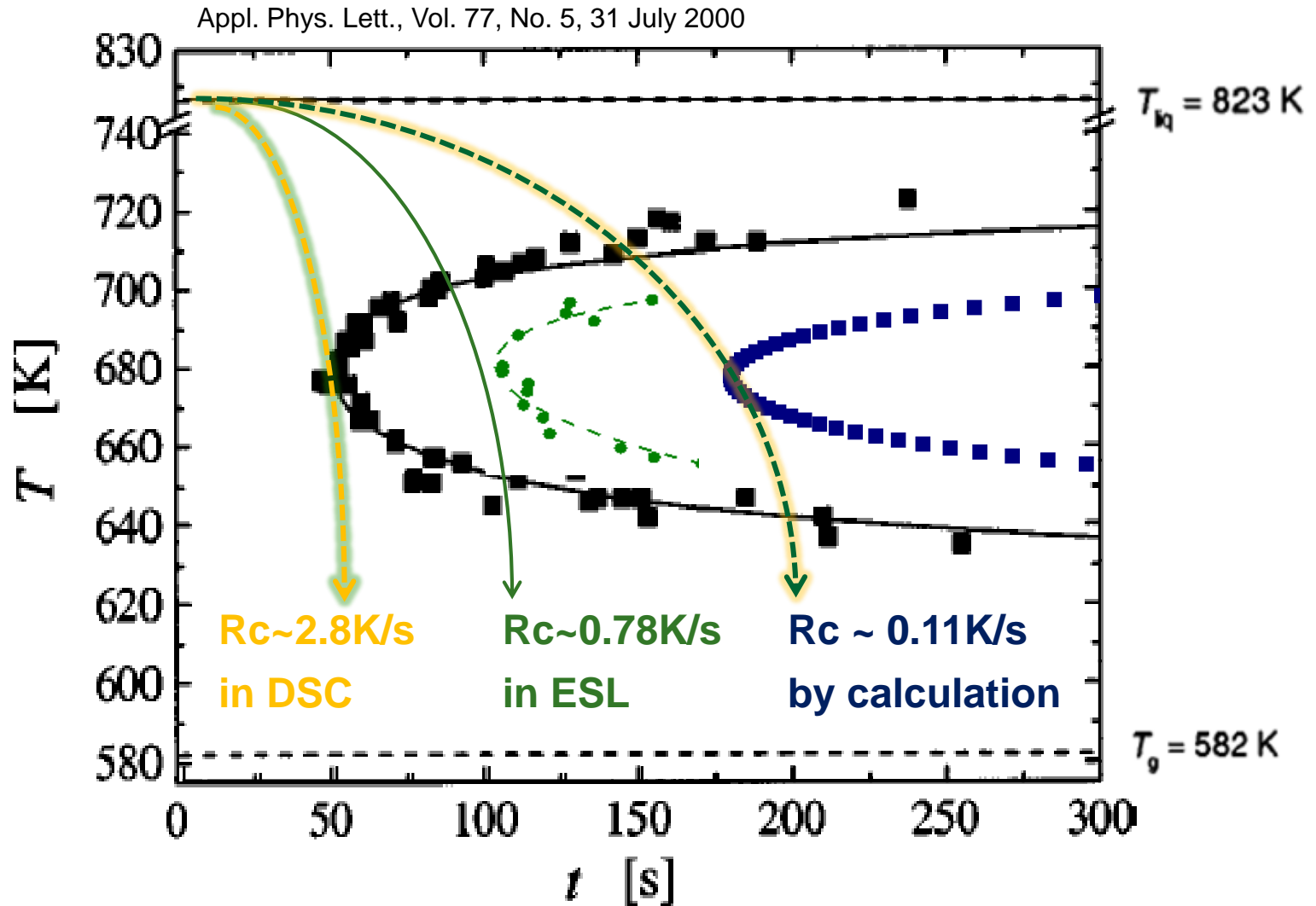


# TTT Diagram of Pd<sub>42.5</sub>Ni<sub>7.5</sub>Cu<sub>30</sub>P<sub>20</sub>





# TTT Diagram of Pd<sub>40</sub>Cu<sub>30</sub>Ni<sub>10</sub>P<sub>20</sub>



## 2.6 Methods to Synthesize Metallic Glasses

### 2.6.1 Vapor-state Processes: expensive & slow, electronic & magnetic applications

#### Thermal Evaporation/ Sputtering/ Vapor Chemical Deposition



### 2.6.2 Liquid-state Processes : Rapid Solidification Process (RSP) $10^{5-6}$ K/s most ideal way to obtain metallic glasses, especially the bulk foam

#### Splat Quenching/ Melt-spinning/ Electro Deposition/ Gas Atomization

### 2.6.3 Solid-state Processes\_Solid state diffusional amorphization

**Mechanical Alloying & Milling/ Hydrogen-induced Amorphization/  
Multilayer Amorphization/ Pressure-induced Amorphization/  
Amorphization by Irradiation/ Severe Plastic Deformation\_Intense  
deformation at low temperatures /Accumulative Roll Bonding (ARB process)**

## 2.6 Methods to Synthesize Metallic Glasses

### 2.6.1 Vapor-state Processes: expensive & slow, electronic & magnetic applications

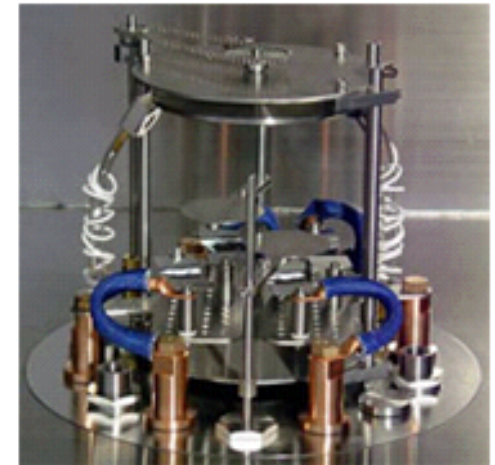
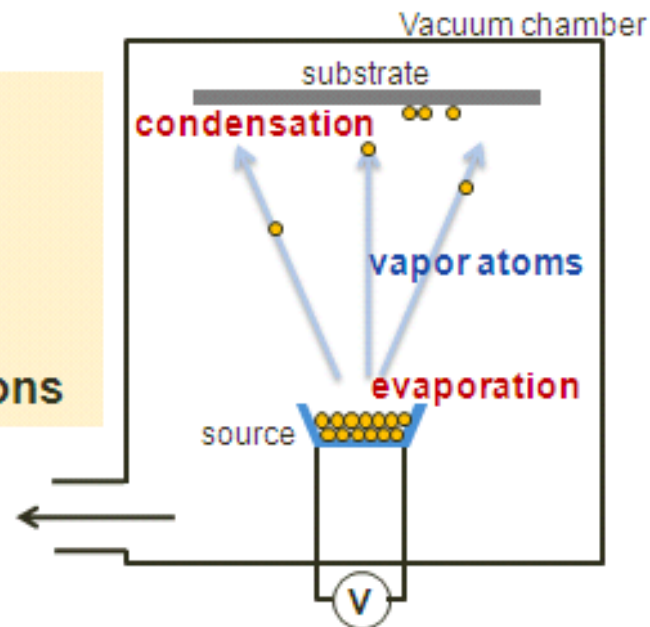
#### A. Thermal Evaporation

Surface coating

- ❖ Thermal evaporation is a common method for thin film deposition.
- ❖ The source material is **evaporated** from a source by heating in a **vacuum**.
- ❖ The evaporated material is then **condensed** on the substrate.

**Vacuum** : evaporated particles can travel directly to the substrate

**Mean free path** :  
~ chamber dimensions



**Heating** : resistance heating (Joule effect)

# First Amorphous Metals: evaporation method

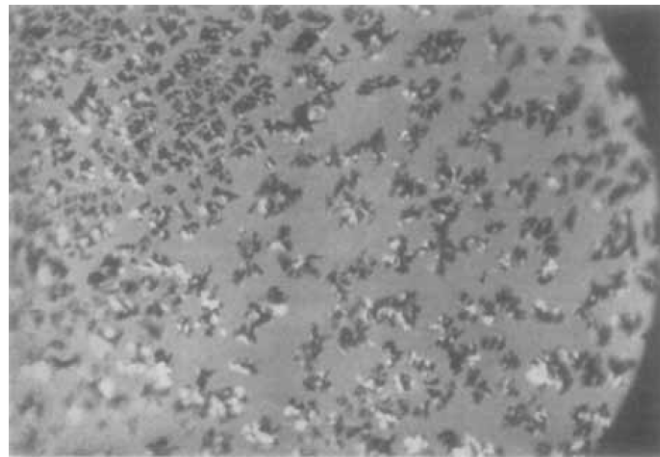
## Über nichtleitende Metallmodifikationen<sup>1)</sup>

Von Johannes Kramer

(Mit 8 Figuren)

Das metallische Leitvermögen wird bekanntlich auf das Vorhandensein freibeweglicher Elektronen und damit auch ortsgebundener positiver Ionen zurückgeführt. Da nun ein nichtionisierter Metaldampf ein vollkommener Nichtleiter ist, so liegt die Vermutung nahe, daß es bei Kondensation eines solchen Dampfes gelingen müßte, nichtleitende Schichten zu erhalten, wenn Wechselwirkungen zwischen den regellos aufeinandergepackten Atomen vermieden werden könnten. Man hätte es dann mit einem Gebilde zu tun, das als völlig amorph anzusehen wäre und in seiner Konstitution am ehesten einem hochkomprimierten Gase entspräche.

J. Kramer  
Nonconducting modifications  
of metals.  
Ann. Physik (Berlin,  
Germany) 19, 37 (1934)



Sb metal → Bi, Ga, and Sn-Bi alloys

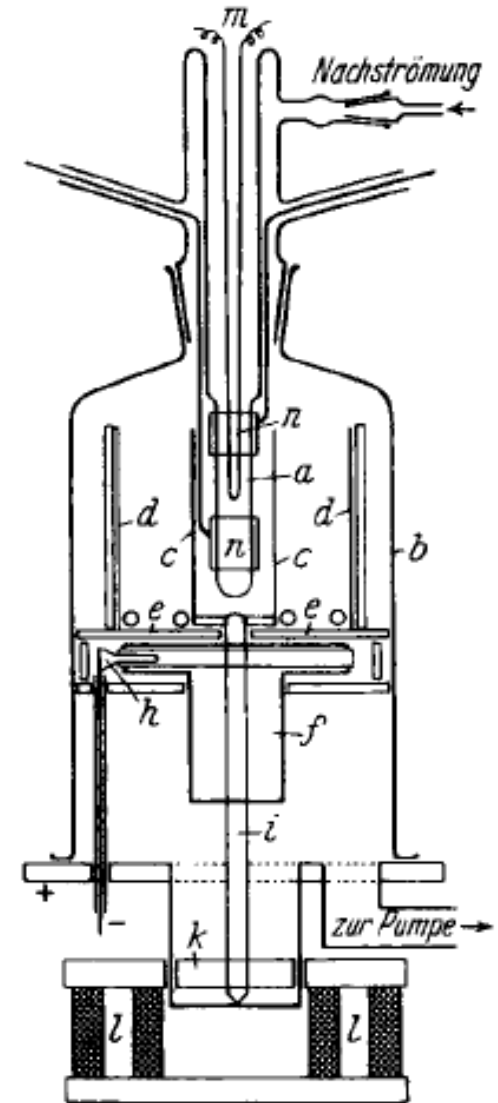


Fig. 1.  
Zerstäubungsapparatur

## 2.6.1 Vapor-state Processes

# What is Sputtering?

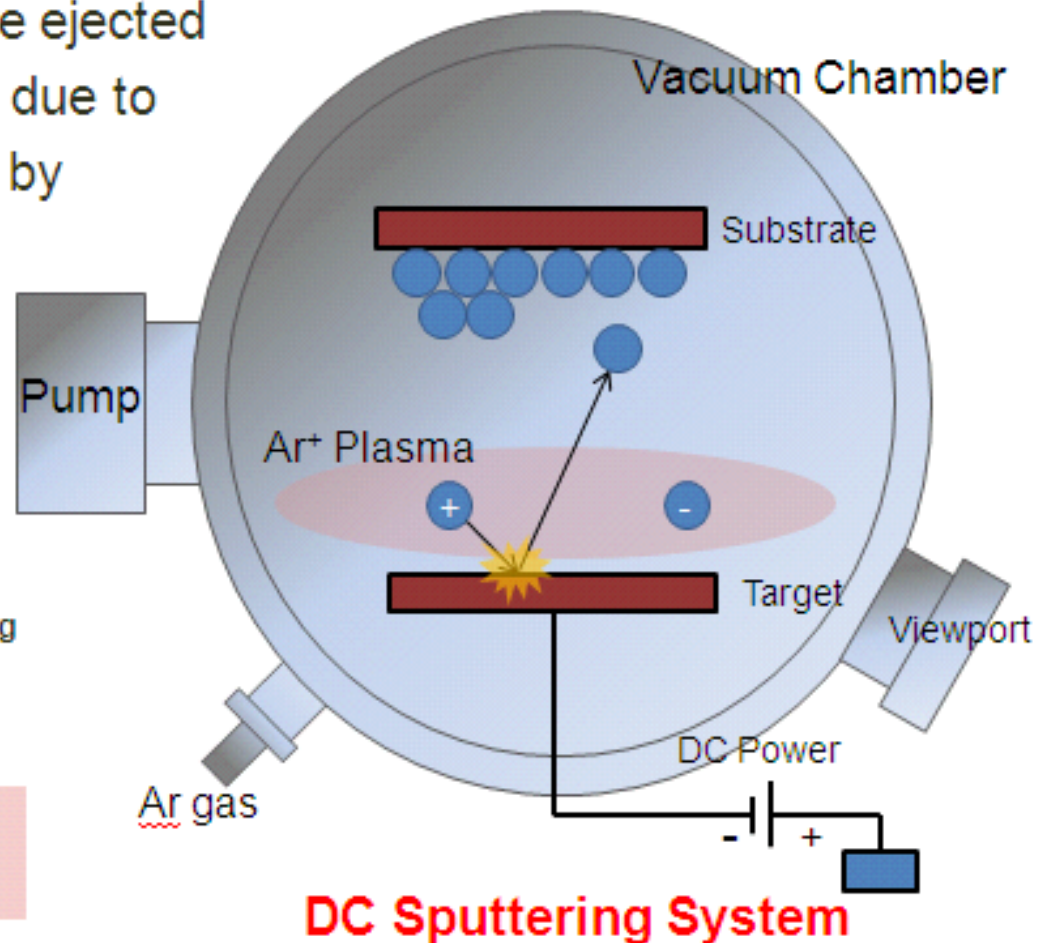
Surface coating

**B. Sputtering** is a common method for thin film deposition.

- ❖ Process whereby atoms are ejected from a solid target material due to bombardment of the target by energetic particles.
- ❖ Ejected atoms are deposited on the substrate, form thin film.

Ref. <http://en.wikipedia.org/wiki/Sputtering>

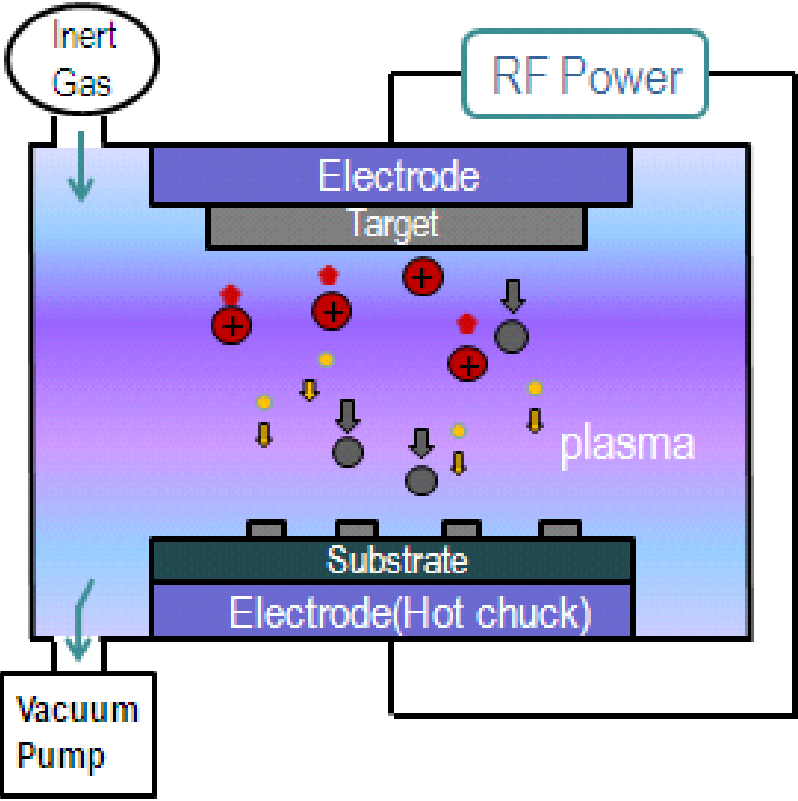
**Vacuum** : evaporated particles can travel directly to the substrate



# 2.6.1 Vapor-state Processes

## Radio Frequency Sputtering

Surface coating



- Neutral target atom
- + Ionized atom
- Electron

### ✓ DC vs RF

	DC Sputter	RF Sputter
Deposition rate	faster	slower
Inert Gas Pressure	Higher	lower
Dep.material	Metal	Metal, Insulator, oxide
ETC		Improve plasma handling.

### ✓ Controlling Temperature of Chuck

Cooling rate of the thin film can be modulated.



Some of materials can formed to amorphous state.

Ex) Crystallinity of ZnO  $\propto \frac{1}{\text{Chuck temp}}$

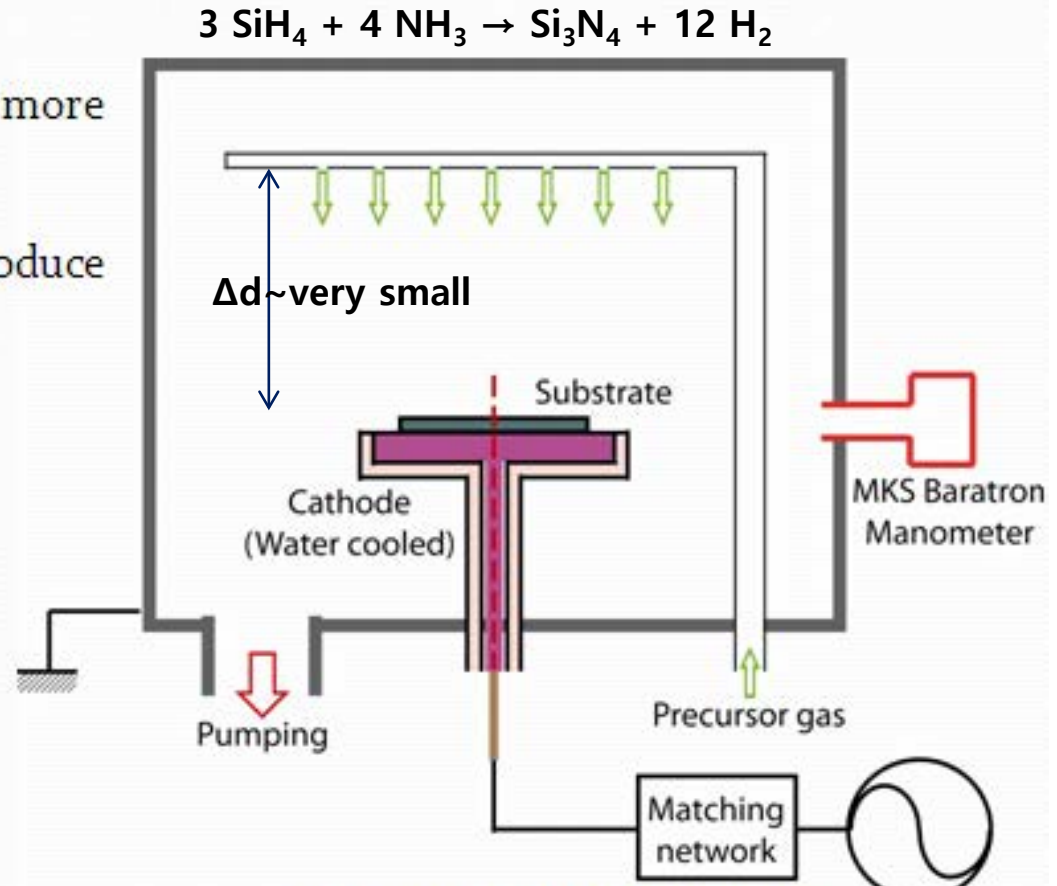


# 2.6.1 Vapor-state Processes

## C. Principles of CVD

### Surface coating

- Substrate is exposed to one or more volatile precursors.
- Precursors will react and/or decompose on substrate to produce the desired deposit.



A schematic of r.f. PACVD coating chamber.

- Base and deposition pressure:  $10^{-6}$  and  $10^{-2}$  Torr
- Bias voltage: -400 to -800V
- Deposition temp. : RT



- PECVD (Plasma Enhanced CVD)
- LPCVD (Low Pressure CVD)
- APCVD (Atmospheric Pressure CVD)
- UHVCVD (Ultra-high vacuum CVD)
- DLICVD (Direct liquid injection CVD)
- AACVD (Aerosol-assisted CVD)
- MPCVD (Microwave Plasma CVD)
- ALCVD (Atomic Layer CVD)
- Laser CVD

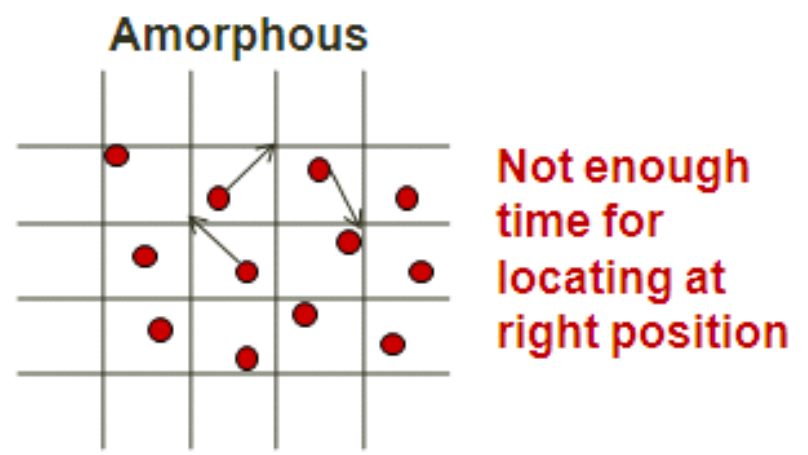
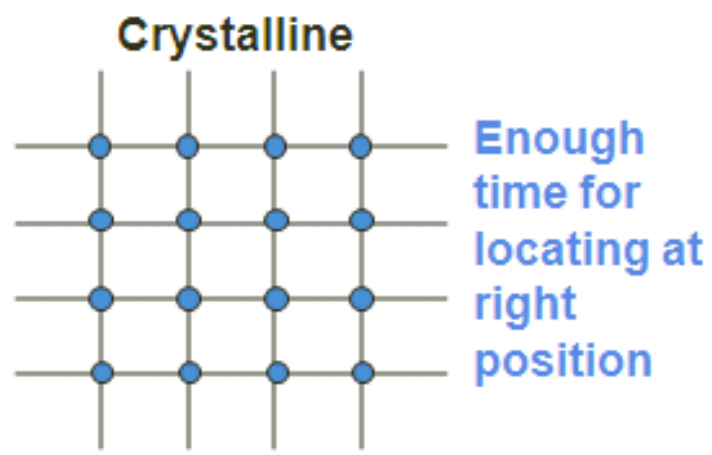


# 2.6.1 Vapor-state Processes

## Formation of Amorphous Thin Film

Surface coating

### Calculation of Diffusion Length



$$l \equiv \sqrt{Dt} \equiv \sqrt{D_0 \exp\left(-\frac{Q_s}{kT}\right) \frac{1}{\text{dep rate}}}$$

Diffusion length (points to  $l$ )

Diffusivity (points to  $D_0$ )

Lifetime of monomer (points to  $t$ )

Deposition condition (T, dep rate) affects the diffusion length



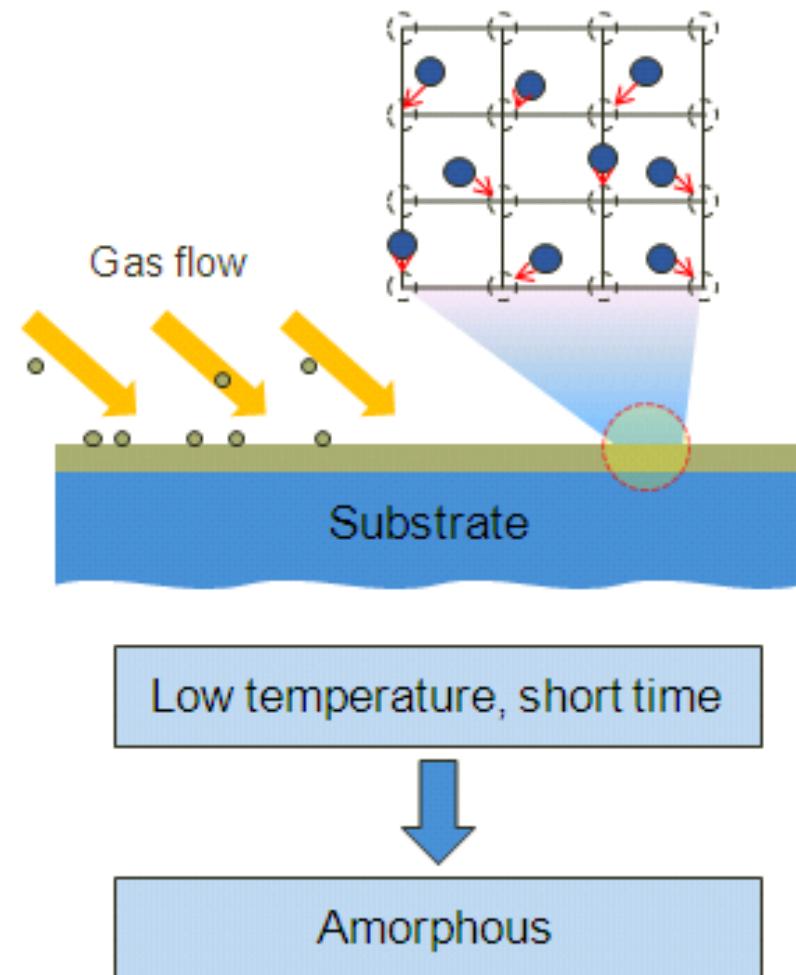
Diffusion length determines the crystallinity of thin film

## 2.6.1 Vapor-state Processes

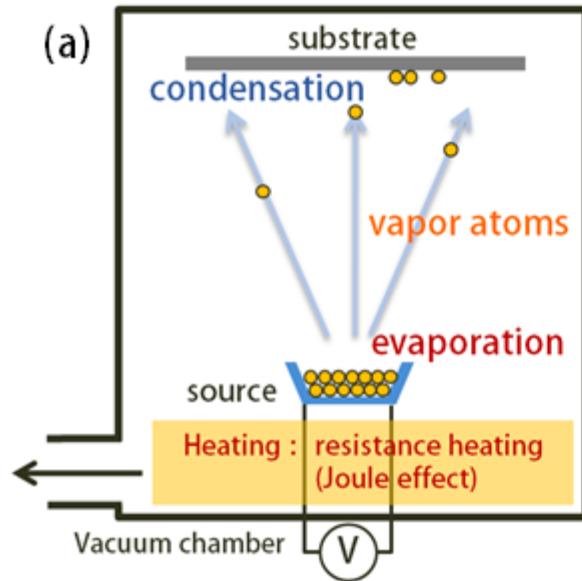
# Formation of amorphous

Surface coating

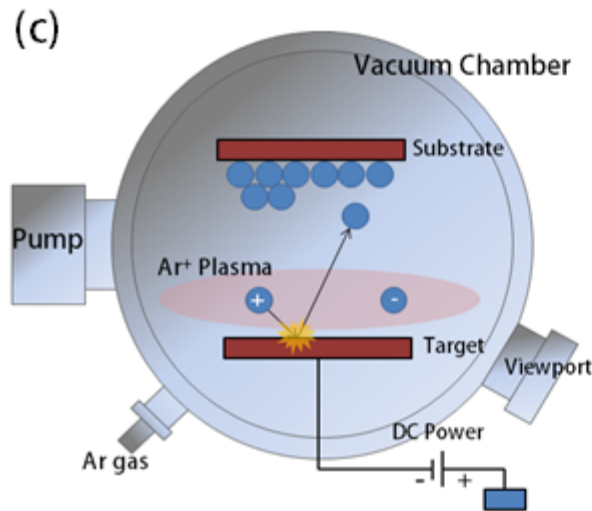
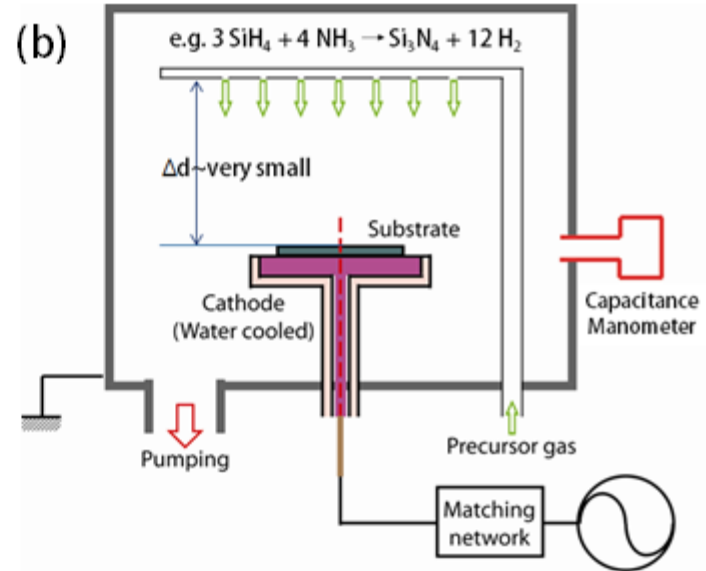
- ❖ Amorphous forming ability is depends on **diffusion length**
- ❖ Diffusion length  $\propto \sqrt{Dt}$
- ❖ Deposit process is commonly forming amorphous because of low temperature and rapid growth rate
- ❖ CVD process is progressed at little high temperature, so metal do not forming amorphous generally



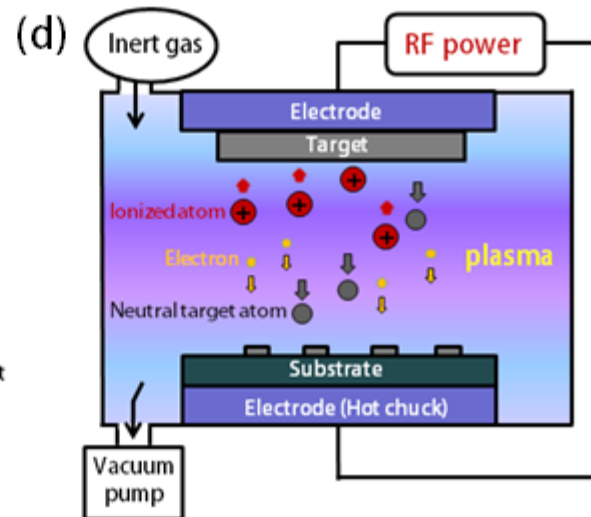
# Chemical vapor deposition



# Sputtering



Electron beam evaporation

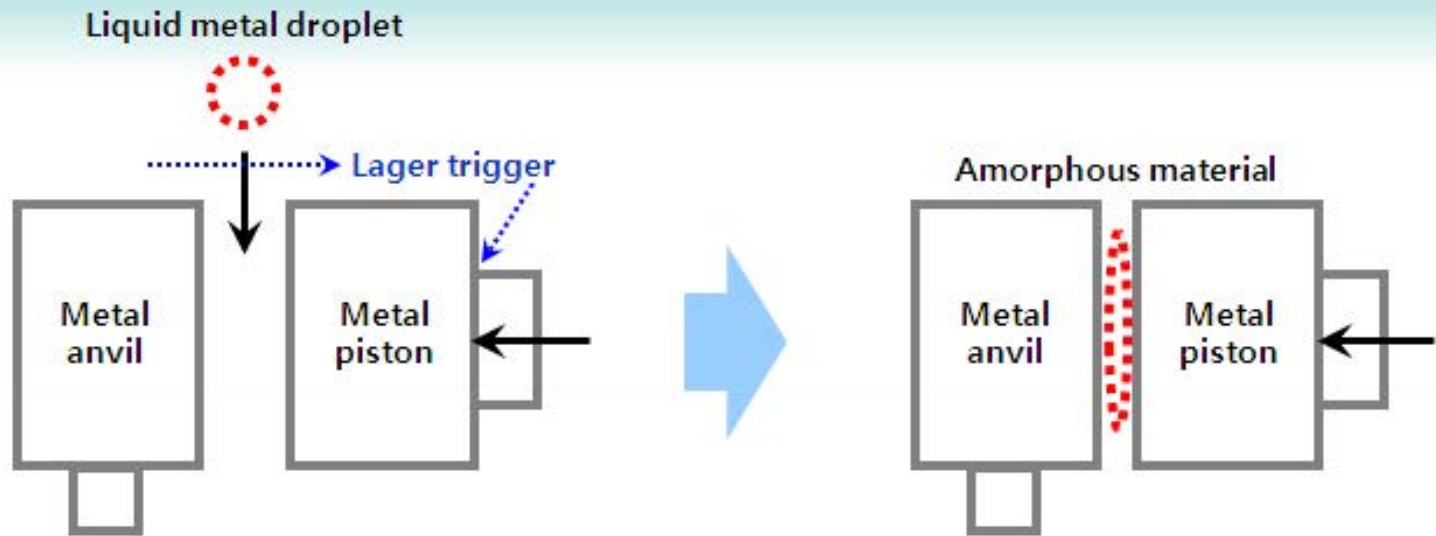


Ion implantation

## 2.6.2 Liquid-state Processes : Rapid Solidification Process (RSP) $10^{5-6}$ K/s most ideal way to obtain metallic glasses, especially the bulk variety

### A. Procedure of Splat Quenching

Thin plate



Liquid metal droplet drops



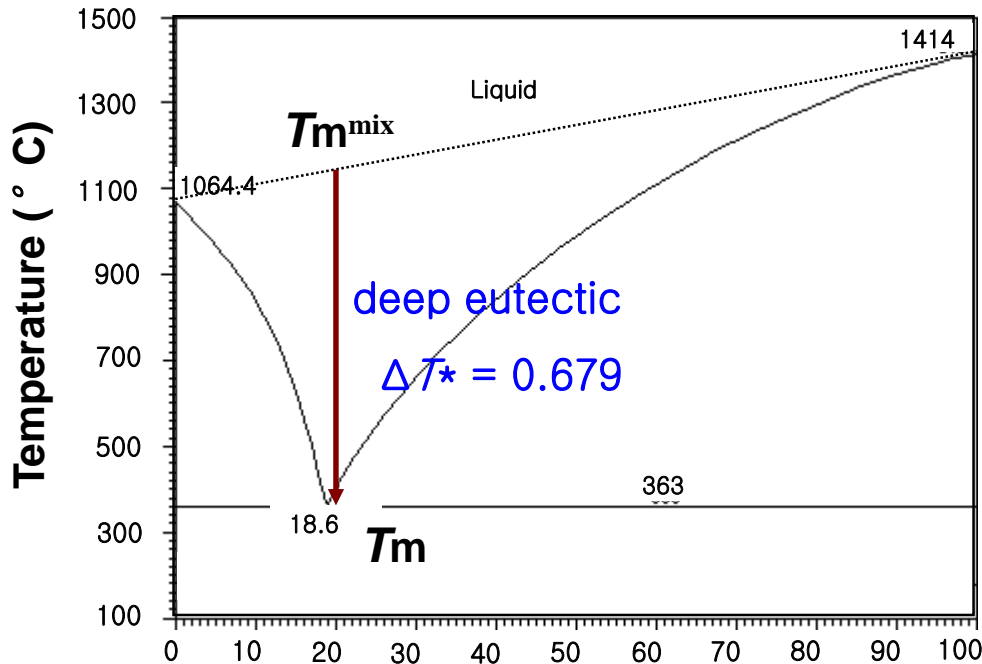
Laser reheats this liquid metal  
& signals to sensor for moving piston



liquid metal is quenched  
& transformed to  
amorphous material

# Glass formation : stabilizing the liquid phase

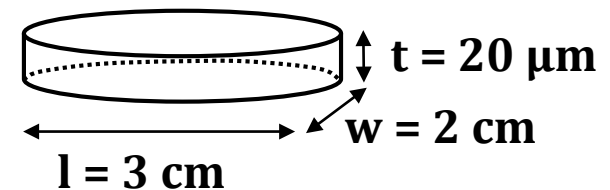
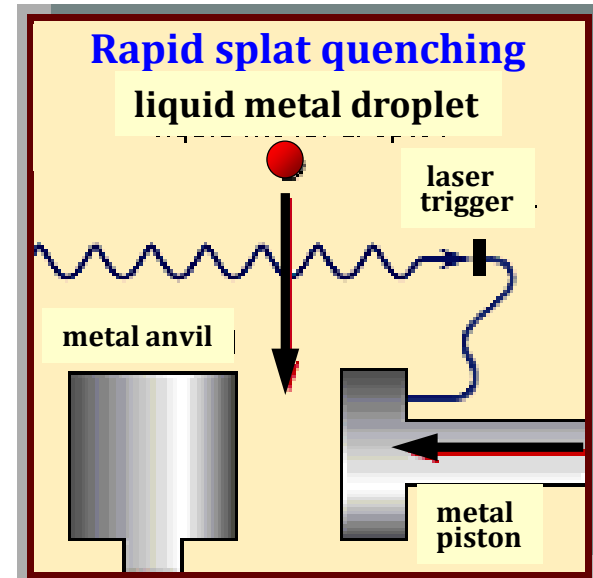
- ▶ First **metallic glass** ( $\text{Au}_{80}\text{Si}_{20}$ ) produced by splat quenching at Caltech by Pol Duwez in 1960.



Au

Si

*W. Klement, R.H. Willens, P. Duwez, Nature 1960; 187: 869.*



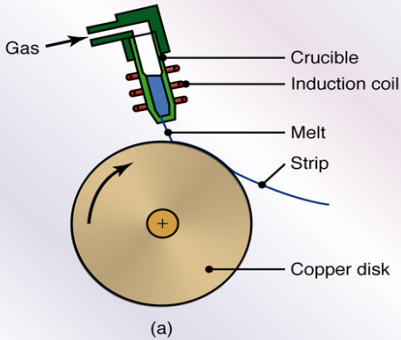
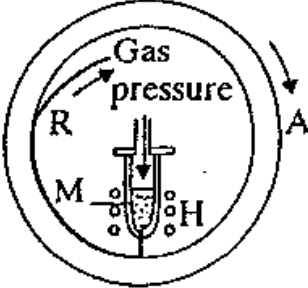
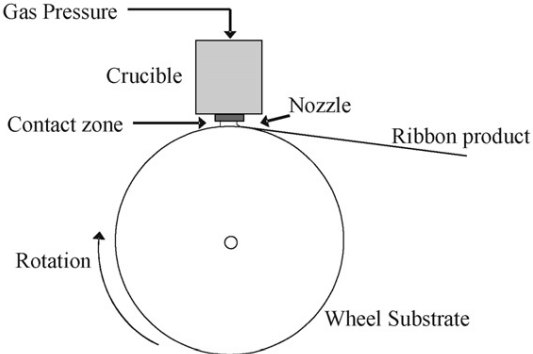
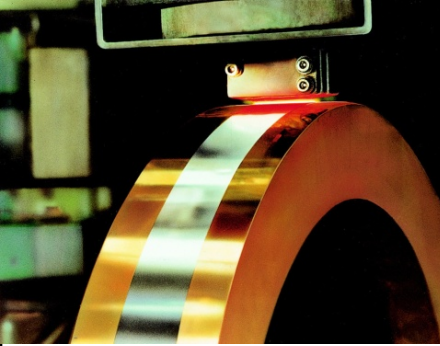
## 2.6.2 Liquid-state Processes

### B.   Brief Definition of Melt Spinning

Thin film

A jet of liquid metal is ejected from a nozzle and impinges on the surface of a rotating substrate, where a thin layer is formed from a melt puddle and rapidly solidifies as a continuous ribbon.

### Several Types of Melt Spinning Method

Free Jet Melt spinning (FJMS)		Planar Flow Melt spinning (PFMS)	Example (PFMS, Siemens)
Outside of Wheel	Inside of Wheel		
 <p>(a)</p>			

- **Melt-spinning method**

**Thin film**





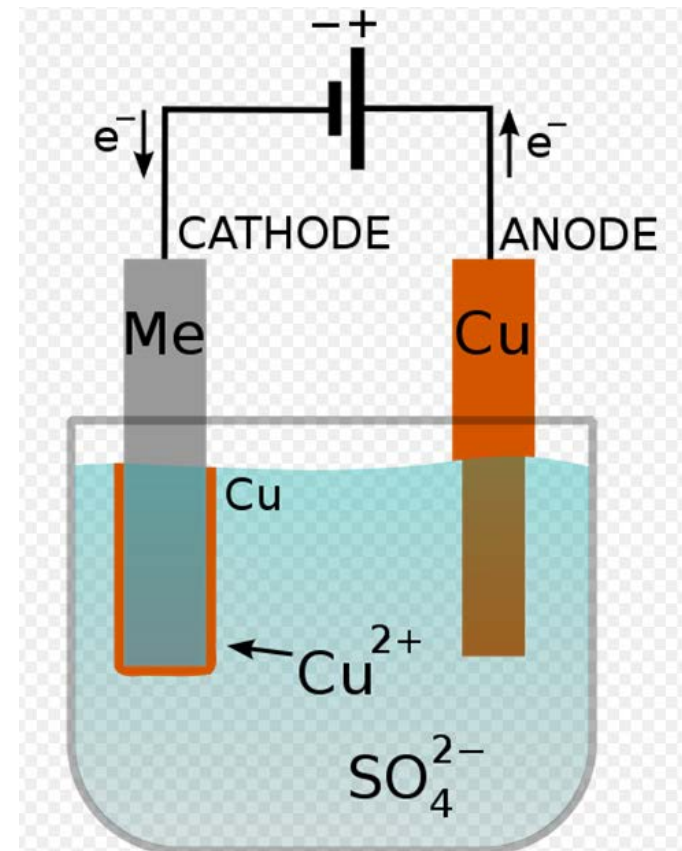
## 2.6.2 Liquid-state Processes

### Surface coating



### C. Basic Concept of Electrolytic Deposition

Electroplating is a plating process in which metal ions in a solution are moved by an electric field to coat an electrode. The process uses electrical current to reduce cations of a desired material from a solution and coat a conductive object with a thin layer of the material, such as a metal. Electroplating is primarily used for depositing a layer of material to bestow a desired property (e.g., abrasion and wear resistance, corrosion protection, lubricity, aesthetic qualities, etc.) to a surface that otherwise lacks that property. Another application uses electroplating to build up thickness on undersized parts. However, the limited size of the product formed in one experiment puts a limitation on the usefulness of this technique to produce large quantities of metallic glasses





## 2.6.2 Liquid-state Processes

### C. Electro-deposition Methods

It was in 1950, for the first time, that Brenner et al. [38] reported the formation of an amorphous phase in electro-deposited Ni–P alloys containing >10 at.% P. The amorphous nature of the deposit was inferred from the presence of only one broad diffuse peak in the XRD pattern. These alloys have a very high hardness and consequently these are used as wear- and corrosion-resistant coatings [39].

U. S. Department of Commerce  
National Bureau of Standards

Research Paper RP2061  
Volume 44, January 1950

Part of the Journal of Research of the National Bureau of Standards

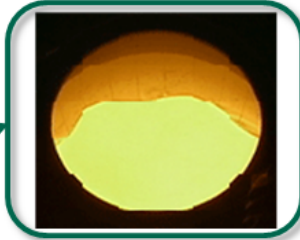
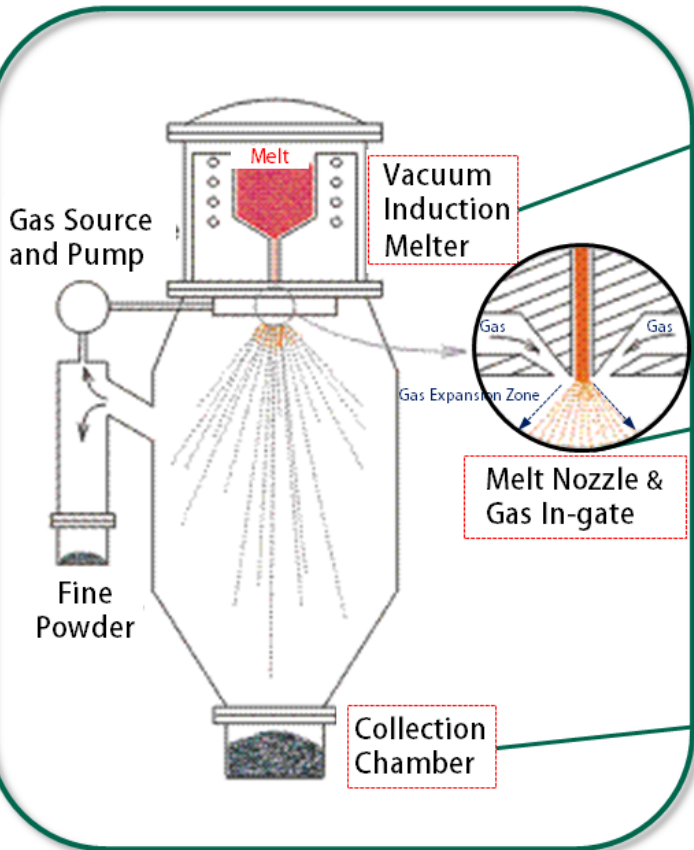
---

## Electrodeposition of Alloys of Phosphorus with Nickel or Cobalt

By Abner Brenner, Dwight E. Couch, and Eugenia Kellogg Williams

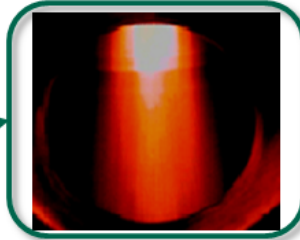
Alloys containing nickel or cobalt and as much as 15 percent of phosphorus have been electrodeposited from solutions containing phosphites. The alloys are hard and may be further hardened by heat-treating at 400° C. The high-phosphorus nickel alloy is more resistant to attack by hydrochloric acid than pure nickel deposits. The high-phosphorus alloys are bright as deposited, but their reflectivities are lower than those of buffed coatings of pure nickel.

# D. Gas Atomization



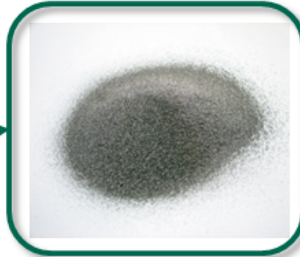
## ■ Melting Furnace Facility

Melting of Metal or Ceramics



## ■ Melt Nozzle and Gas In-gate

A rapidly expanding gas breaks up the liquid stream → thin sheet → ligament → ellipsoid → sphere.



## ■ Collection Chamber

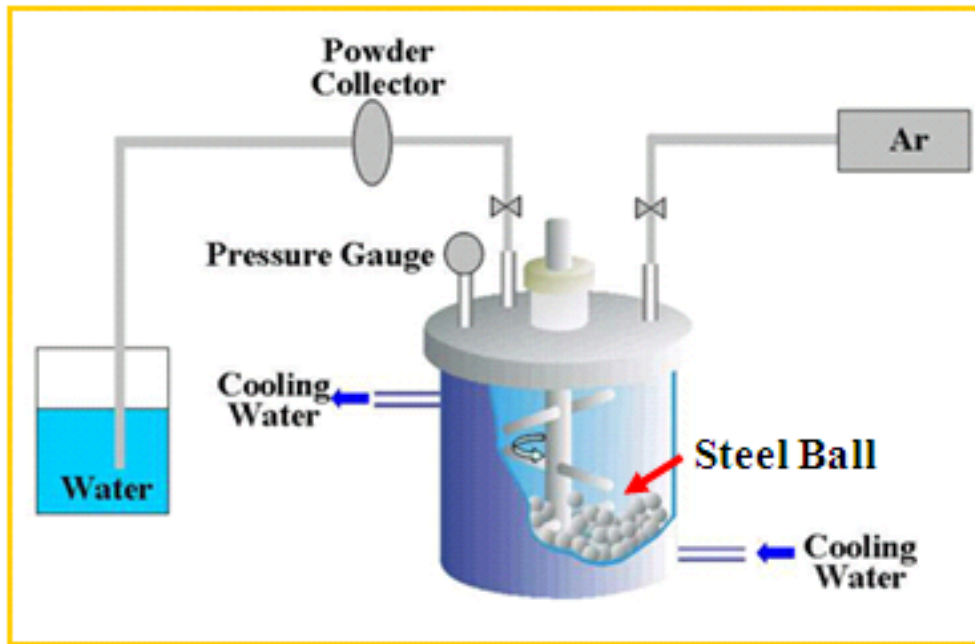
The collection chamber is designed to maximize the yield, minimize contamination, and ease of cleaning.

## 2.6.3 Solid-state Processes

### A. Mechanical alloying/milling

: MA/ MM performed in a high-energy ball mill such as a shaker mill or planetary mill will also induce severe plastic deformation in metals. During milling, particles are fractured and cold welded together, resulting in large deformation.

### Schematic Diagram of Mechanical Alloying Process



Increased Solid Solubility Limit  
Easy to Control the Microstructure  
Easy to Fabricate Non-Equilibrium and Nano Phase  
Homogeneous Distribution of Fine Strengtheners  
Excellent Mechanical Properties



Attritor

## 2.6.3 Solid-state Processes

### A. Mechanical alloying/milling

The milled powder particles experience heavy plastic deformation leading to the generation of a variety of crystal defects such as dislocations, grain boundaries, and stacking faults. These defects raise the free energy of the crystalline system to a level higher than that of a hypothetical amorphous phase, and consequently, the crystalline phase becomes destabilized and an amorphous phase forms [41,42].

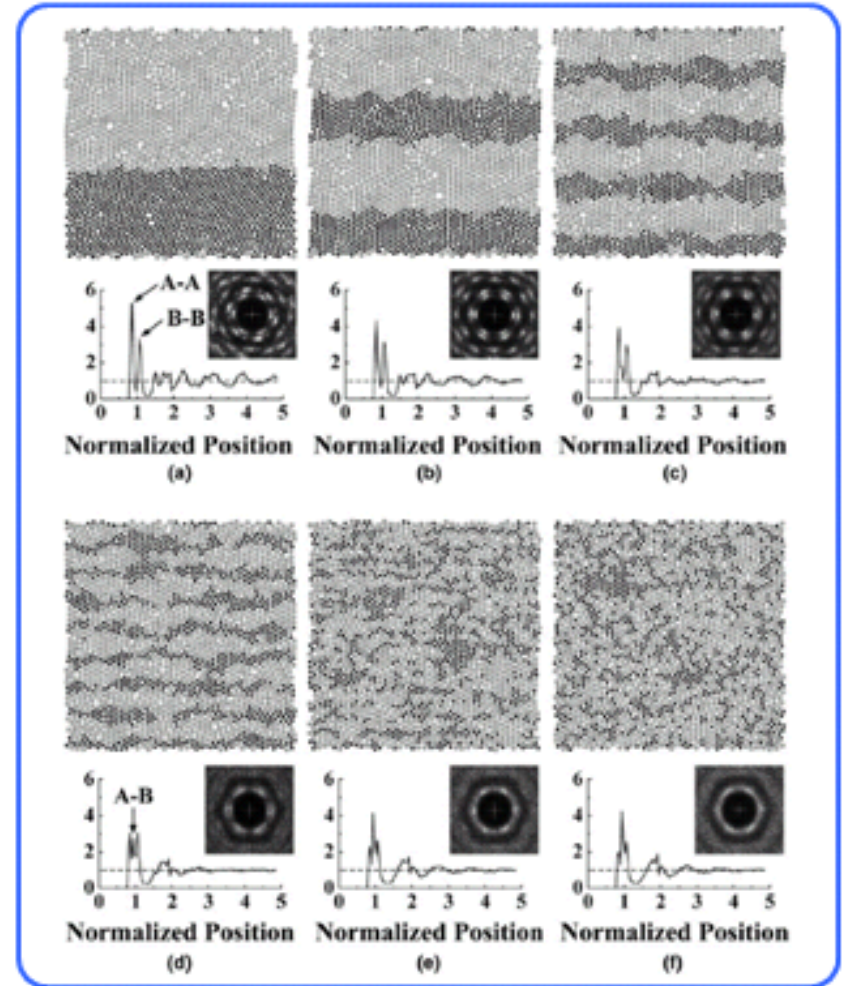
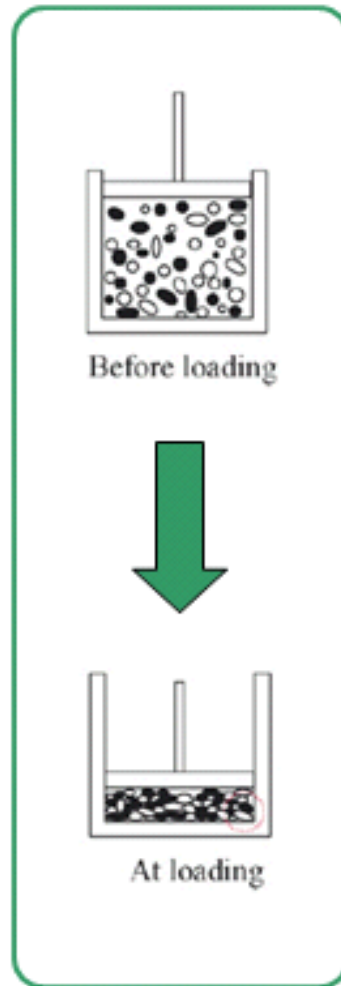
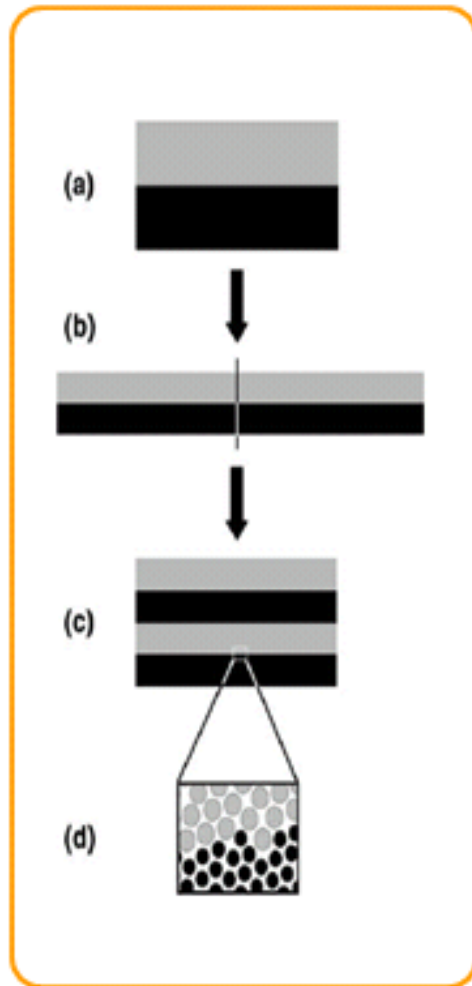
The first report of the formation of an amorphous phase by mechanical milling was in a Y-Co intermetallic compound [43] and that by mechanical alloying in a Ni-Nb powder blend [44]. Subsequently, amorphous phases have been formed in a number of binary, ternary, and higher-order systems by this method. Unlike in RSP methods, the conditions for the formation of an amorphous phase by mechanical alloying/milling seem to be quite different. For example, amorphous phases are formed, not necessarily near eutectic compositions, and in a much wider composition range. The nature and transformation behavior of the amorphous phases formed by mechanical alloying/milling also appear to be different from those formed by RSP.



## 2.6.3 Solid-state Processes

### A. Mechanical alloying/milling

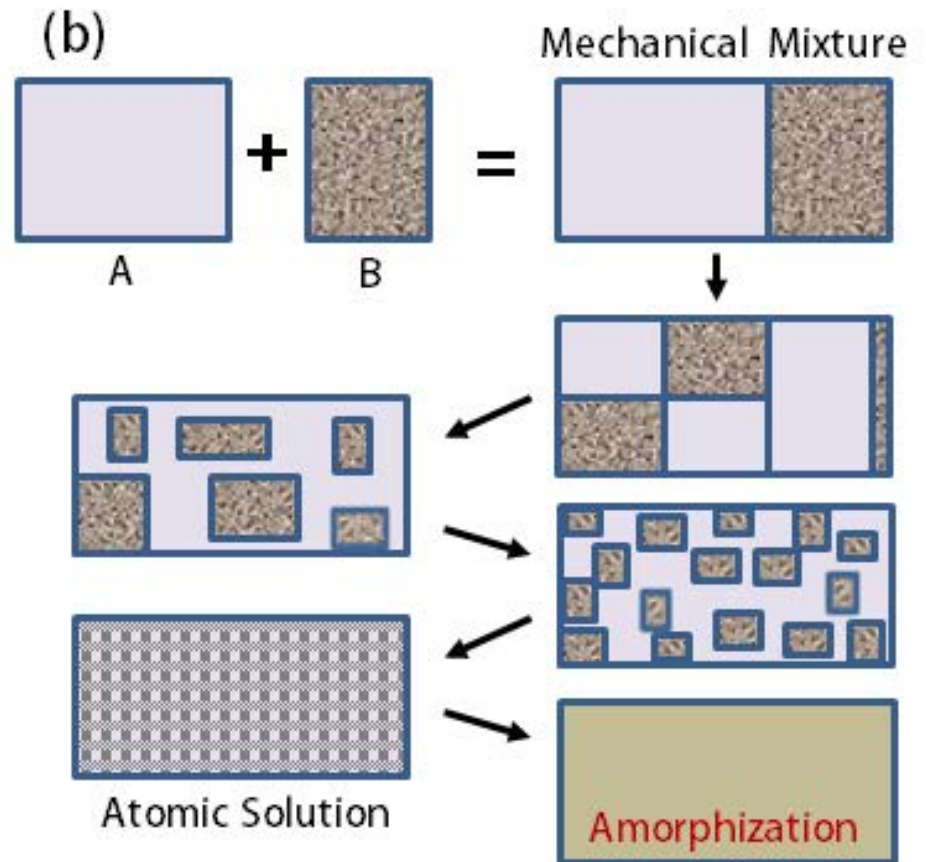
#### Amorphization during Mechanical Alloying



A. C. Lund and C. A. Schuh, *Acta Mater.* Vol. 52 (2004)



# Mechanical Alloying/ Milling



## 2.6.3 Solid-state Processes

### B. Hydrogen-induced Amorphization

- Yeh et al. [45] reported the formation of an amorphous metal hydride  $Zr_3RhH_{5.5}$  by a reaction of hydrogen with a metastable crystalline  $Zr_3Rh$  compound at sufficiently low temperatures (< about 200°C). A similar amorphous hydride phase was also reported to form when the amorphous  $Zr_3Rh$  alloy obtained in a glassy state was also reacted with hydrogen.
- Aoki [46] has reported that hydrogen-induced amorphization is possible in many binary metal compounds.

### C. Multilayer Amorphization

- An amorphous phase was found to form when thin metal films (10–50 nm in thickness) of La and Au were allowed to interdiffuse at relatively low temperatures (50°C–100°C). Similar to the case of hydrogen-induced amorphization, here also the large asymmetry in the diffusion coefficients of the two elements was found to be responsible for the formation of the amorphous phase [47]. Since then, a large number of cases where multilayer amorphization occurs have been reported.

**Ex)** cold rolling of thin foils of Ni and Zr, and then annealing them at a low temperature.

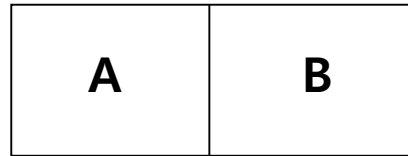
# Solid-State Diffusional Amorphization

- ✓ Alternate layers of crystalline metallic films ('diffusion couples') **interdiffuse** under isothermal conditions, with the eventual amorphization of the **entire** multilayer.
- ✓ **Couple: late transition metal with early transition metal**  
ex. Au-La, Au-Zr, Au-Y, Cu-Zr, Cu-Er, Ni-Er, Ni-Ti, Ni-Hf, Fe-Zr, Co-Zr, Ni-Zr
- ✓ Low temperature annealing **below the crystallization temperature** (the nucleation or growth of crystalline phases cannot occur)

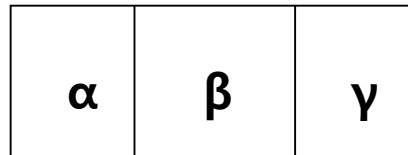


## \* Diffusion in multiple binary system

A diffusion couple made by welding together pure A and pure B

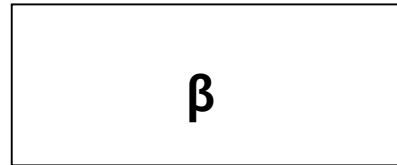


What would be the microstructure evolved after annealing at  $T_1$  ?



→ a layered structure containing  $\alpha$ ,  $\beta$  &  $\gamma$ .

Draw a phase distribution and composition profile in the plot of distance vs.  $X_B$  after annealing at  $T_1$ .

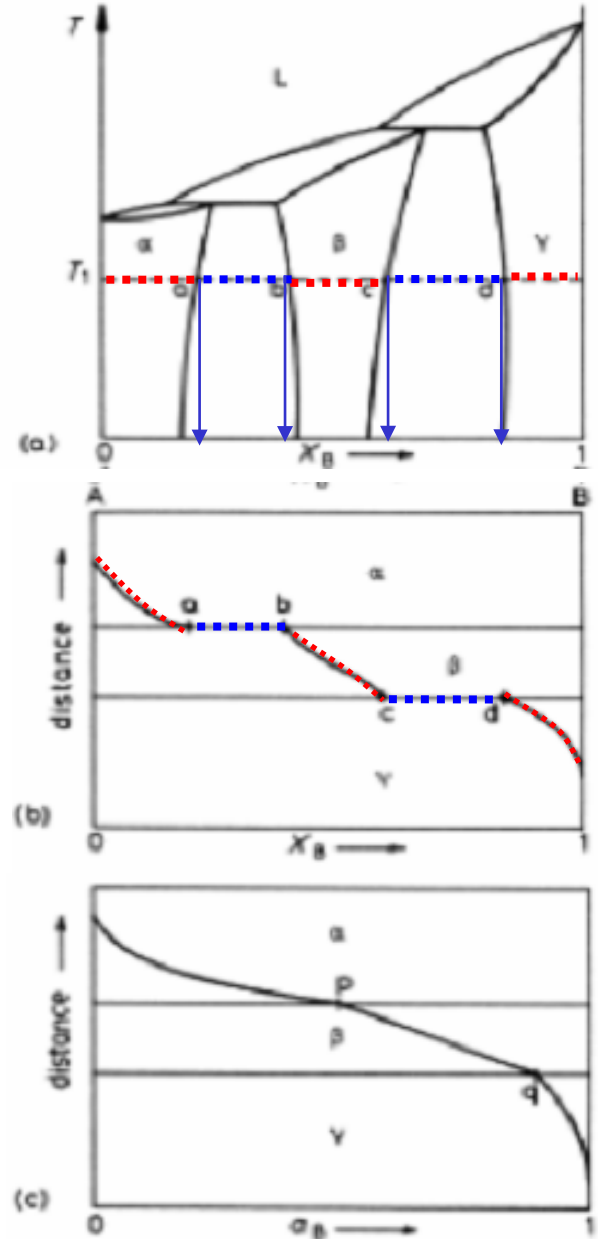


Draw a profile of activity of B atom, in the plot of distance vs.  $a_B$  after annealing at  $T_1$ .

A or B atom → easy to jump interface (local equil.)

$$\rightarrow \mu_A^\alpha = \mu_A^\beta, \mu_A^\beta = \mu_A^\gamma \text{ at interface}$$

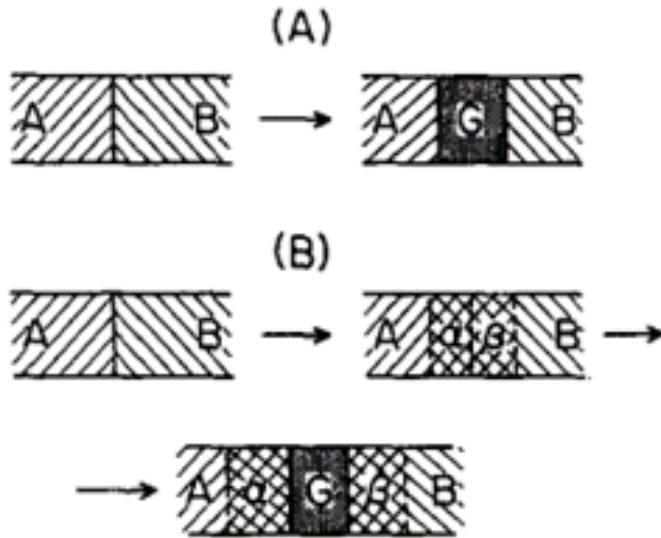
$$(a_A^\alpha = a_A^\beta, a_A^\beta = a_A^\gamma)$$



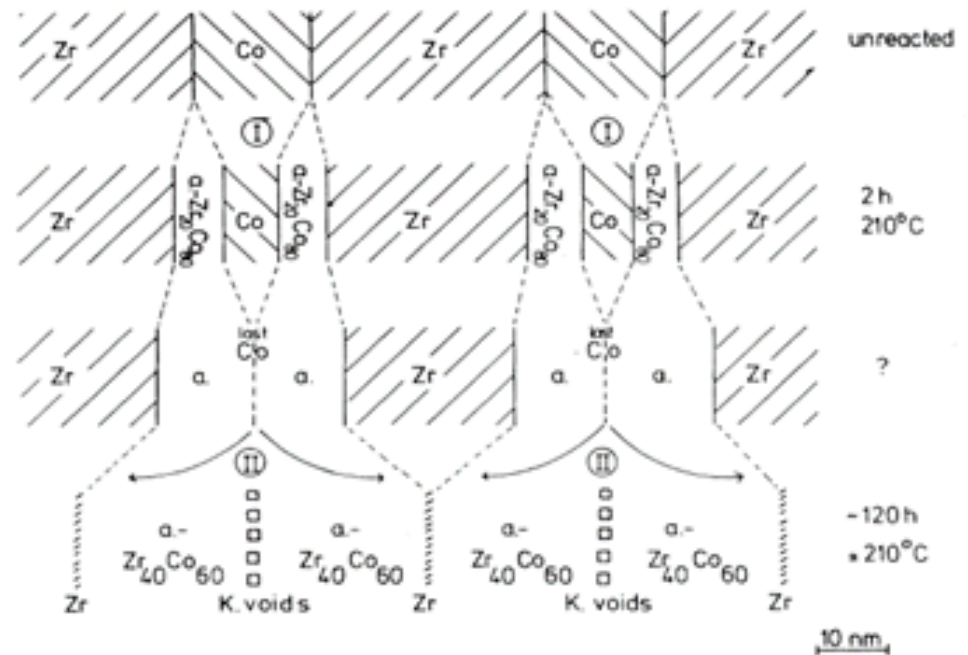
# Solid-State Diffusional Amorphization

## Schematic Diagram

Reaction Paths  
for  
A-B Couple



Example (Co-Zr)

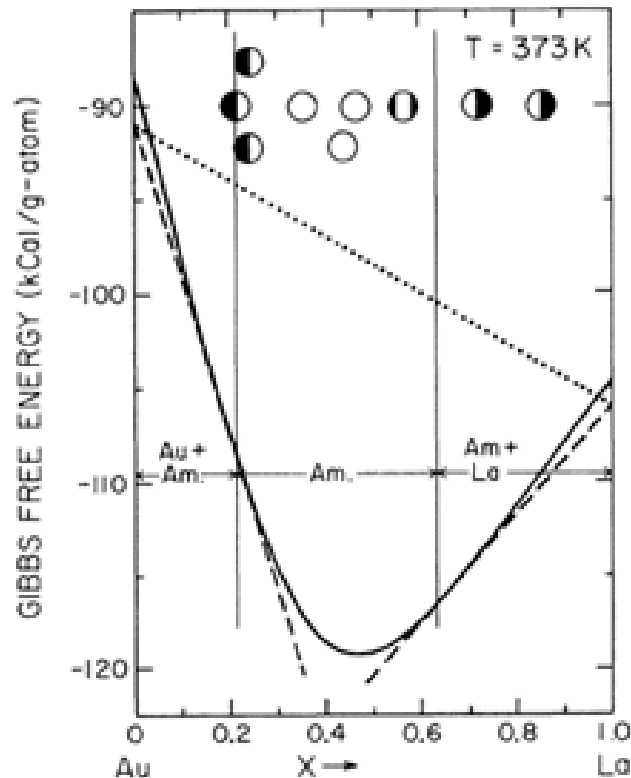


- (A) Direct nucleation of the amorphous phase
- (B) Substantial mutual dissolution of the parent metals leading to unstable solid solutions

# Two Main Attributes

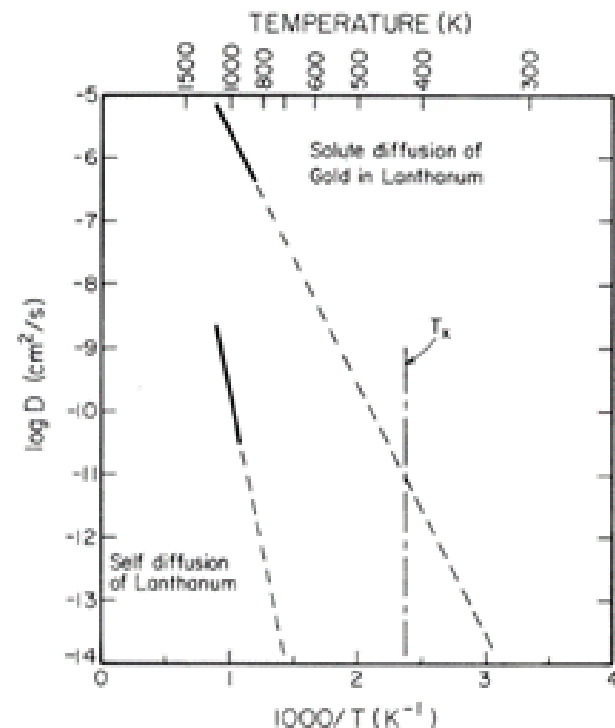
- **A strong thermodynamic driving force**

i.e. a large negative heat of mixing



- **Diffusional asymmetry**

i.e. one element diffuses anomalously fast in the other, but not vice versa



## 2.6.3 Solid-state Processes

### D. Pressure-induced Amorphization

- Alloys in the systems Cd–Sb, Zn–Sb, and Al–Ge were subjected to high pressures when they formed unstable crystalline phases and then decayed in a short time to amorphous phases [50]. An amorphous phase was also found to form in Cu–12–17 at.% Sn alloys when they were heated to high temperatures in a confined pressure, and turning off the power suddenly.

### e. Amorphization by Irradiation

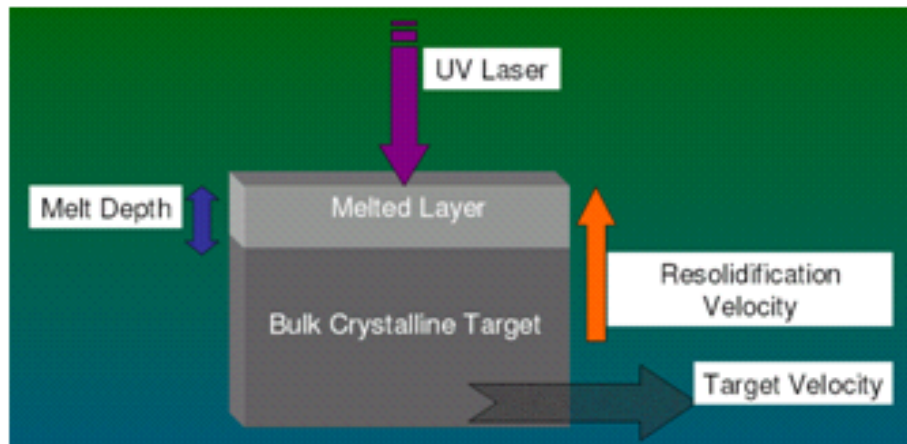
- A number of intermetallics, for example, NiTi, Zr<sub>3</sub>Al, Cu<sub>4</sub>Ti<sub>3</sub>, CuTi<sub>2</sub>, FeTi, etc., have been amorphized by irradiation with high-energy electrons, heavy ions, or fission fragments [18]. It is only intermetallics, and not solid solutions, that have been amorphized this way. Several different criteria have been proposed for this purpose, which include low temperature, high doses, high dose rates, intermetallics with an extremely narrow homogeneity range, permanently ordered compounds (i.e., intermetallics which are ordered up to the melting temperature and do not show an order–disorder transformation), which also have high-ordering energies, destruction of long-range order by irradiation, etc. Fecht and Johnson [52] have analyzed the fundamental issues involved in the amorphization of intermetallics by irradiation methods.

# Preparation of amorphous materials by irradiation

## Two kinds of irradiation effects

- Laser/electron irradiation:

Small area melting  $\rightarrow$  cooling  $\rightarrow$  amorphous layer/crystalline



- Neutron and heavy ion irradiation:

Atomic displacement  $\rightarrow$  recovery  $\rightarrow$  amorphous phase

➤ **Mechanism of irradiation amorphization:**

- The **kinetic knock-off** of atoms from their lattice positions
- Very high temperature is expected in a very small volume during a short time (ps), which causes **melting** of material in a local small point.

➤ **Two opposing radiation-induced processes can be operative:**

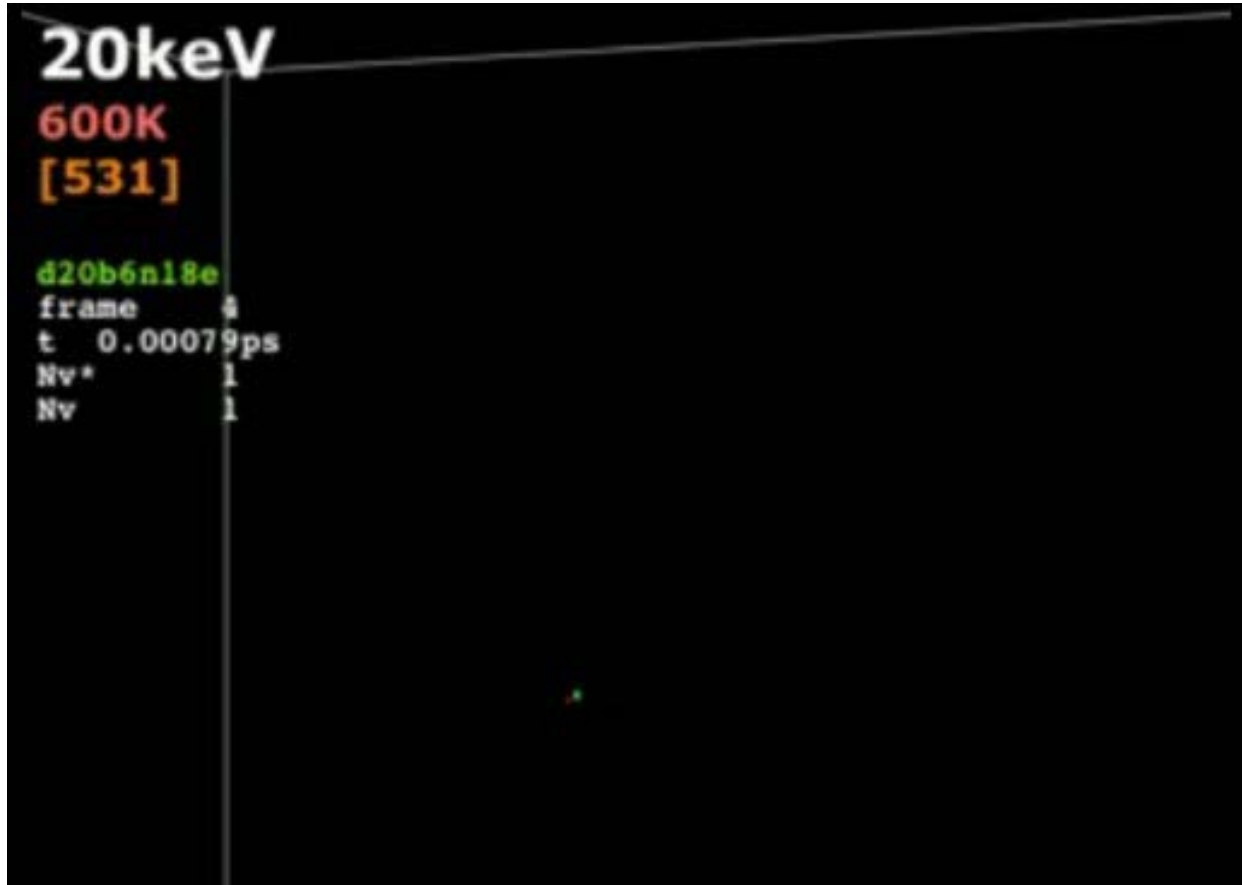
- **Radiation-induced chemical disordering** of atoms on lattice sites will tend to promote amorphization;
- **Radiation-induced defect migration** will tend to restore ordering.

➡ **The irradiation be carried out at sufficiently low temperature to suppress the defect migration.**

**Radiation damage:** damage by collision between high energy particle and materials

► **Basic defect by collision with high E particle: Vacancy & Interstitial**

**(Frenkel pair)**



20keV Fe displacement cascade in bcc Fe at 600K

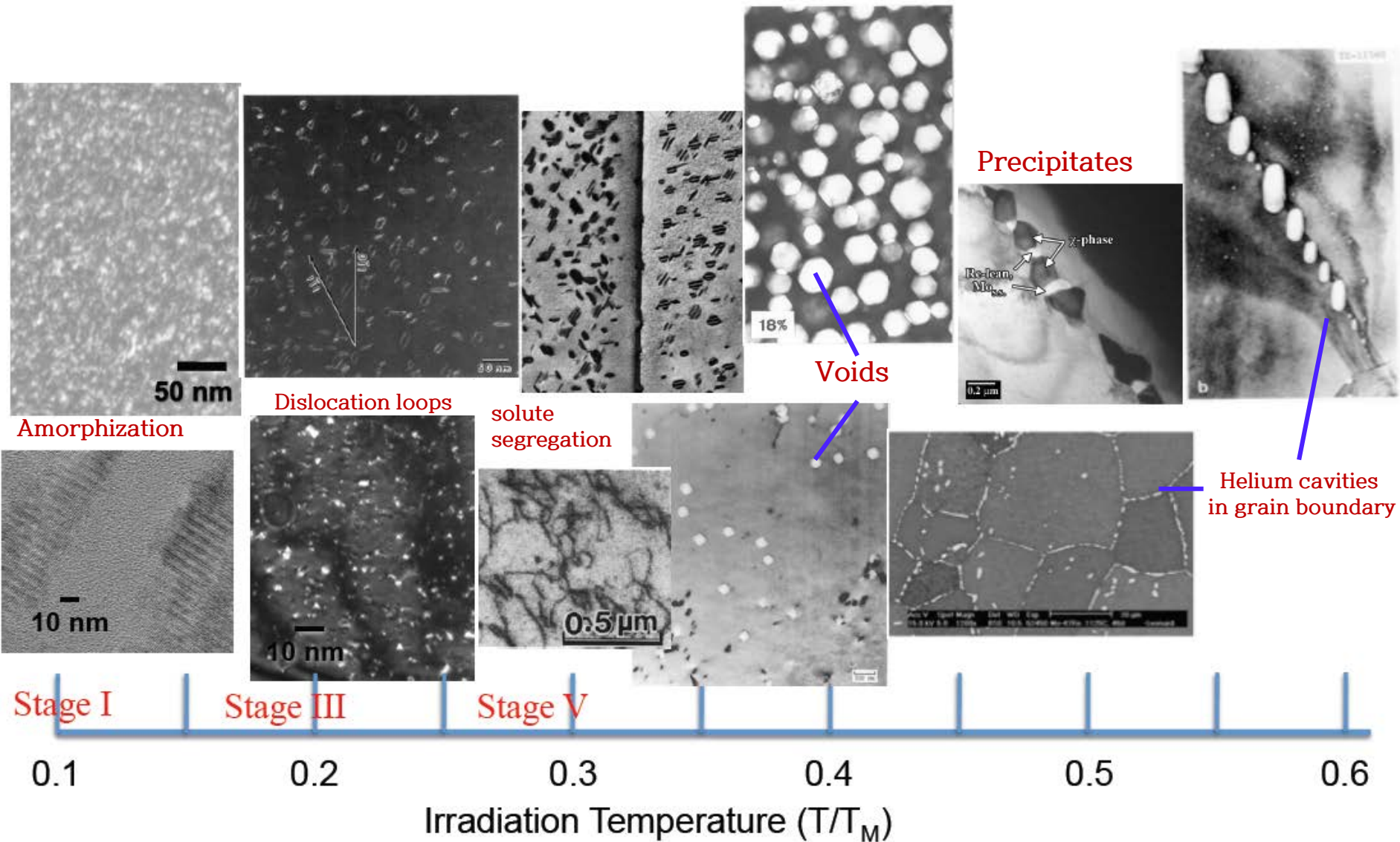
[http://www.youtube.com/watch?v=0btHd\\_8JFV4](http://www.youtube.com/watch?v=0btHd_8JFV4)

\* **A primary knock-on atom (PKA) displaces neighbouring atoms, resulting in an atomic displacement cascade, leading to formation of point defects and defect clusters of vacancies and interstitial atoms.**

Seeger et al., Proc. Symp. Radiat. Damage Solids React. 1 (1962) 101-1056.



# Radiation damage: damage by collision between high energy particle and materials



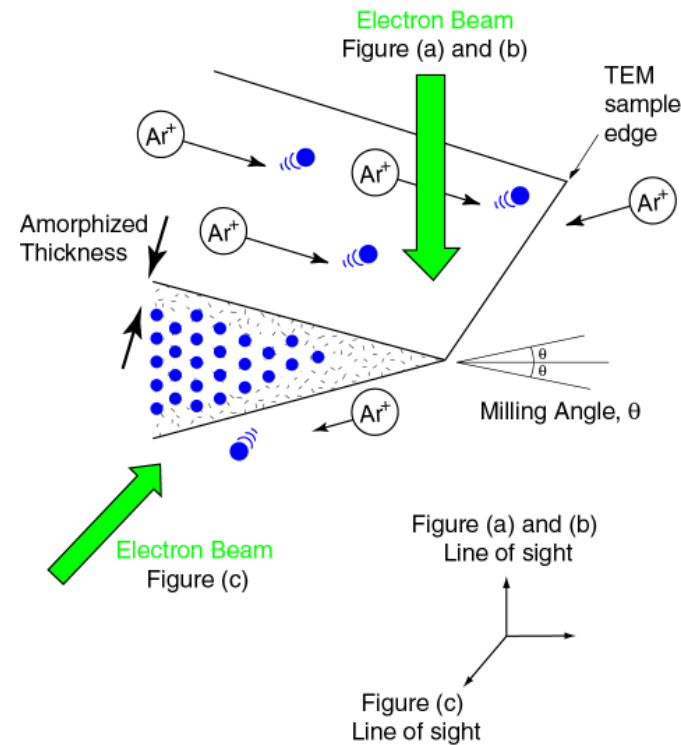
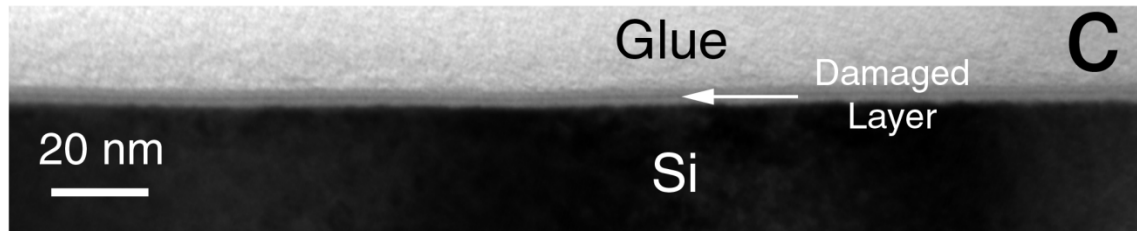
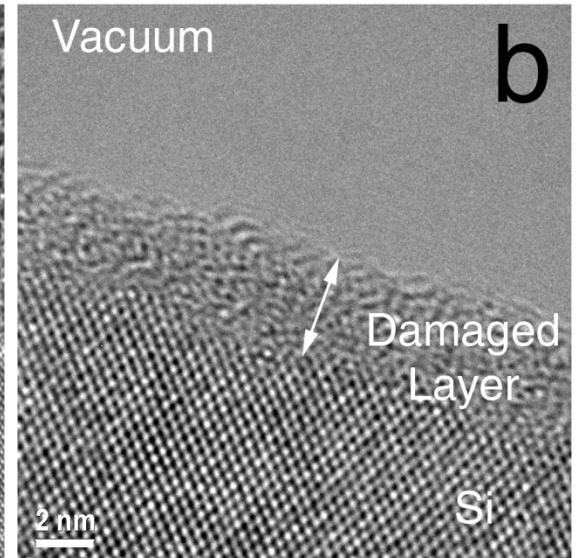
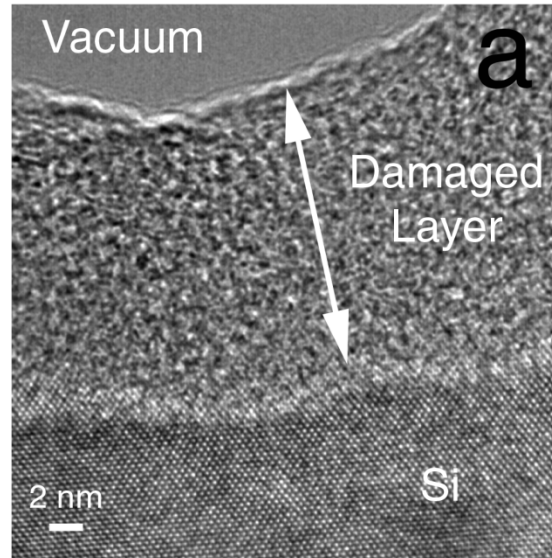


# Sample Preparation : Surface Damage

**Ion beam induced amorphous formation** in Silicon (100)

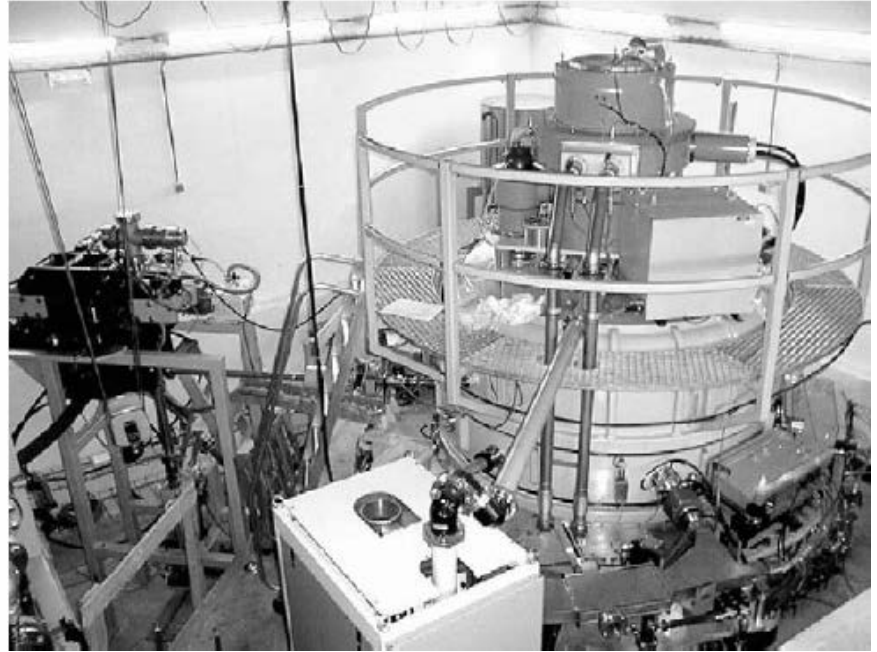
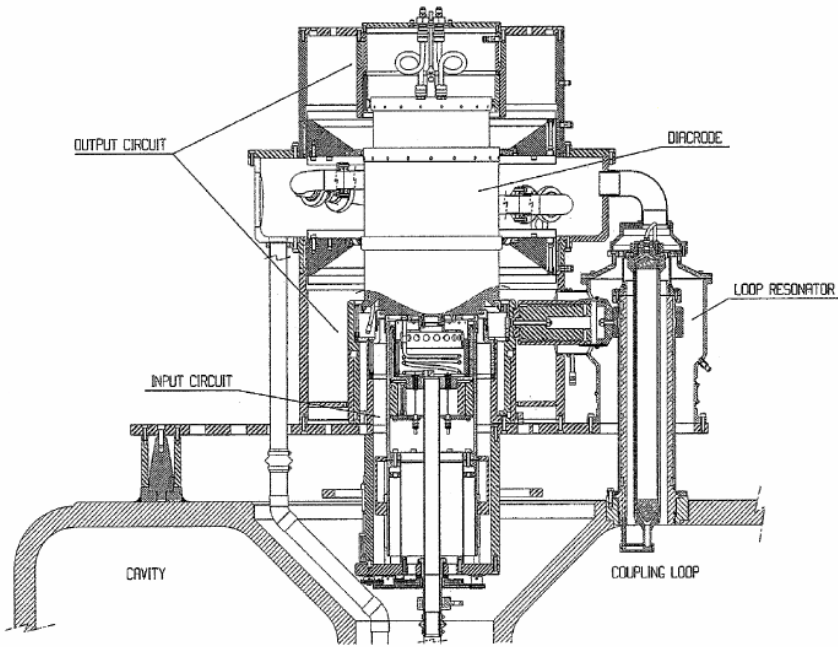
5 keV Ar<sup>+</sup>

250eV Ar<sup>+</sup>

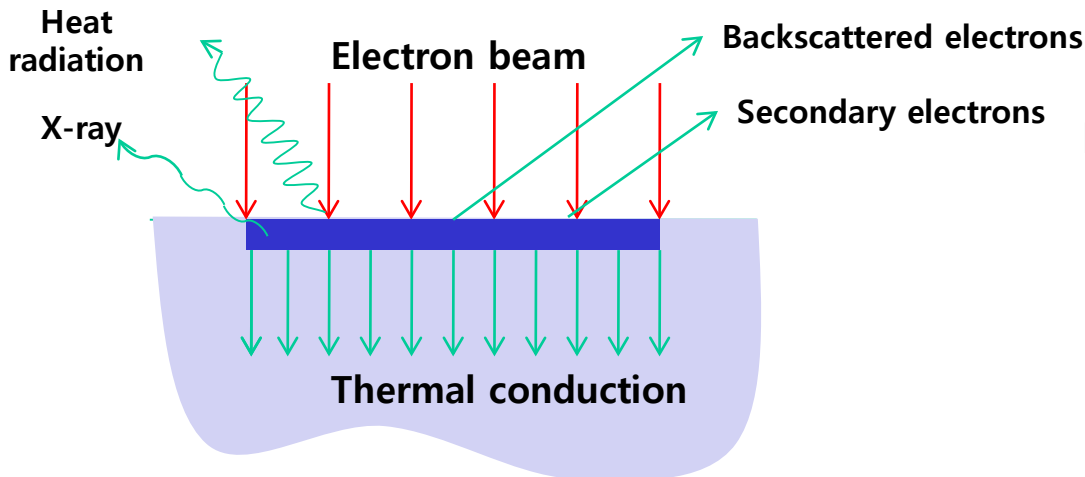


Y.W. Kim, Metals and Materials International, 7, 499 (2001)

# The schematic diagram of High Energy Electron beam accelerator



TT1000 prototype picture

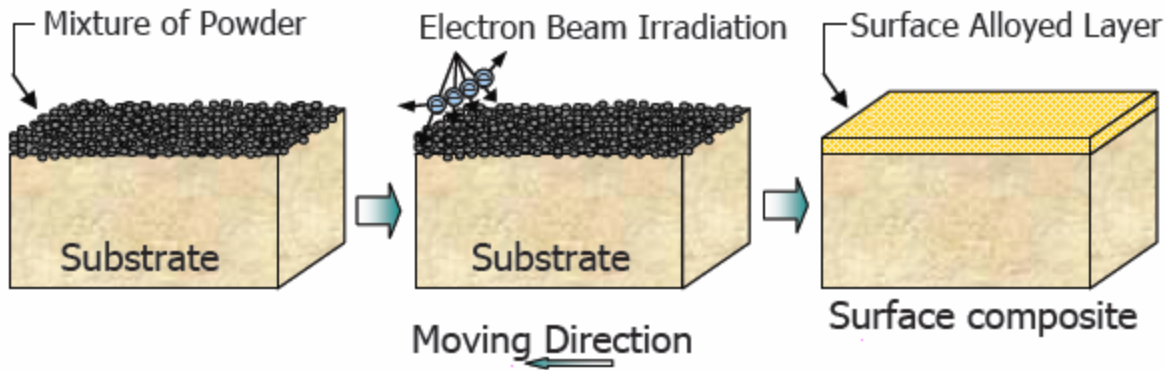


**Kinetic energy of accelerated electron**

**Collided with electrons of materials**

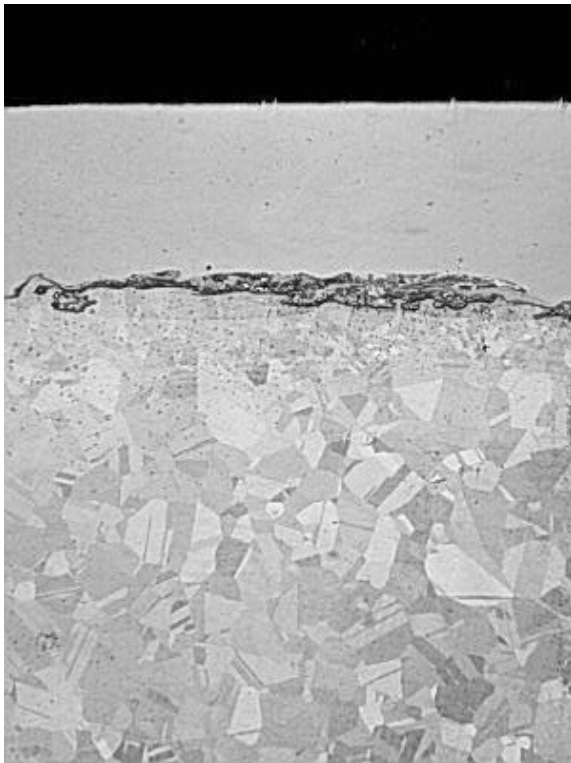
**To transform thermal energy**

# The making method of amorphous materials by Irradiation



❖ Electron beam irradiation is heating the mixture of powder.

❖ The temperature of substrate is so low that surface is super-cooling.



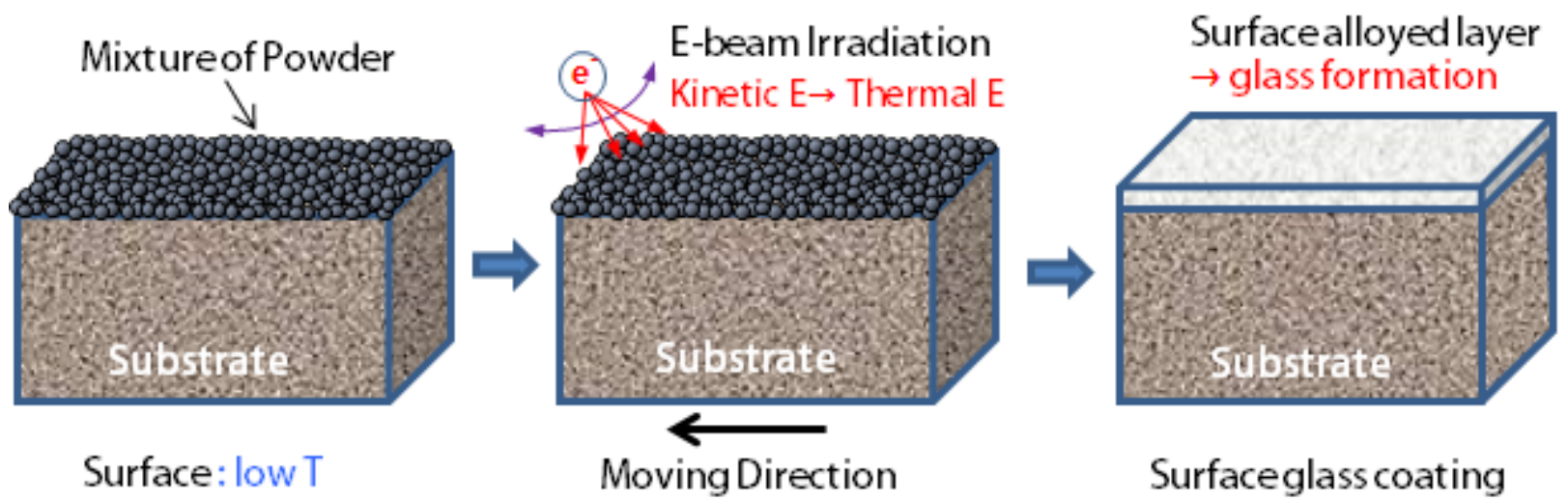
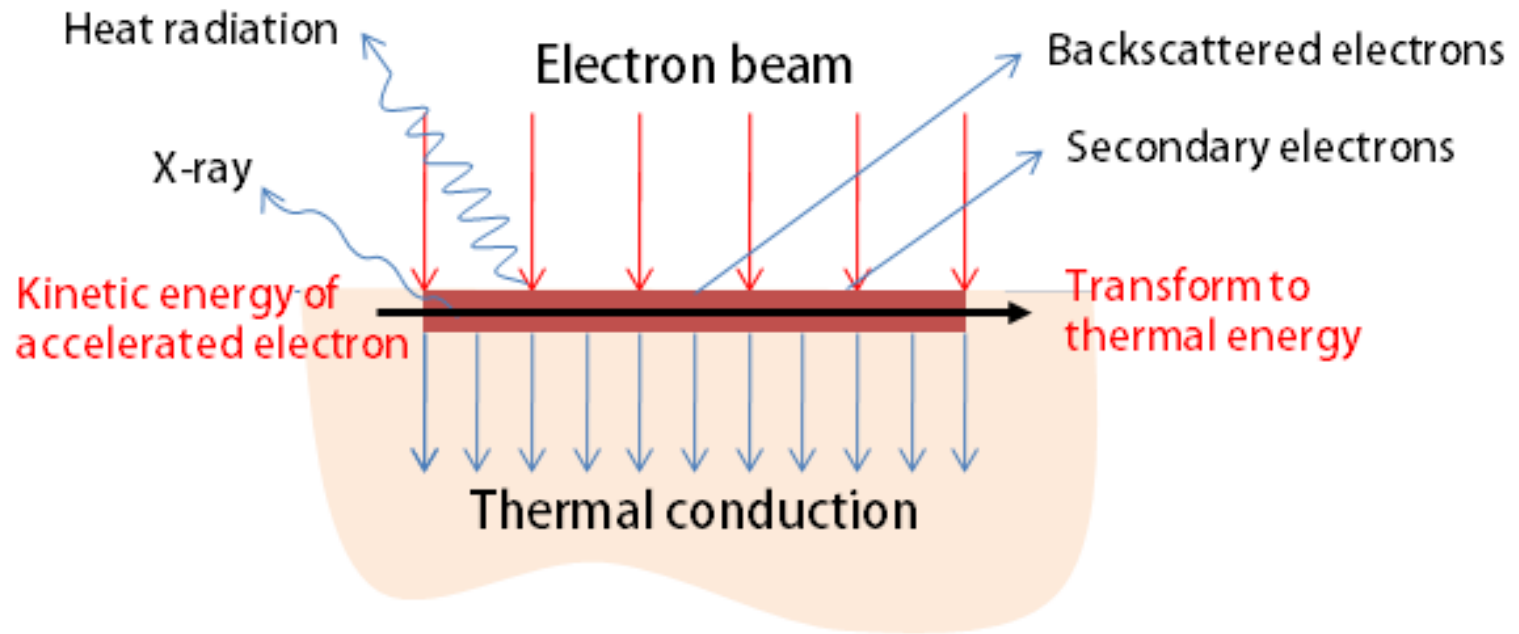
**Surface : Amorphous alloy**

Surface gloss, Hardness, corrosion resistance,

**Substrate : Cu(or Ti, Fe) alloy**

Ductility, limited size of amorphous materials,

It is possible to make mass production and reduce weight

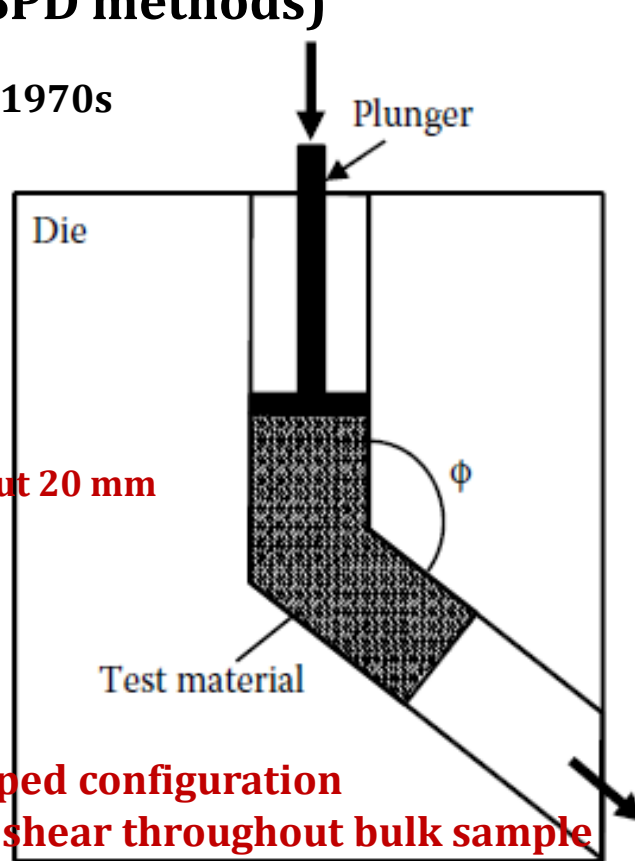




## 2.6.3 Solid-state Processes

### f. Severe Plastic Deformation : Intense deformation at low temperatures (SPD methods)

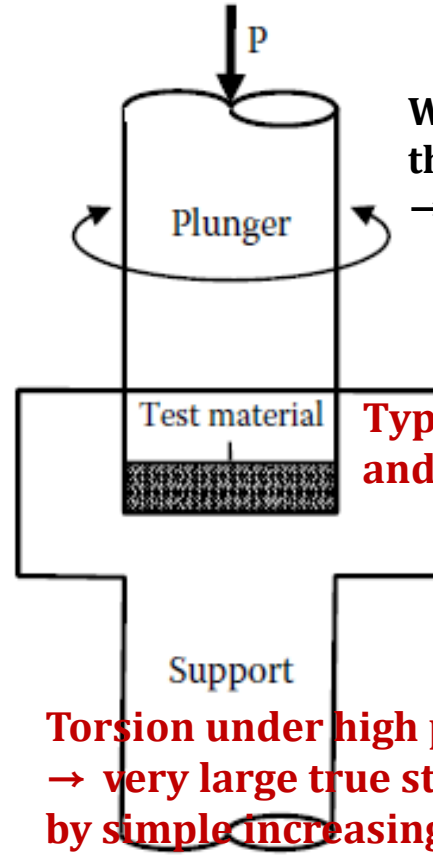
Developed in the 1970s



**Billet diameter**  
~Not exceeding about 20 mm

**Bent into an L-shaped configuration**  
→ Uniform simple shear throughout bulk sample

(a)



Won Percy Bridgman  
the 1946 Nobel prize  
→ metal processing  
~ more recent in 2003

**Torsion under high pressure**  
→ very large true strain  
by simple increasing the # of rotations

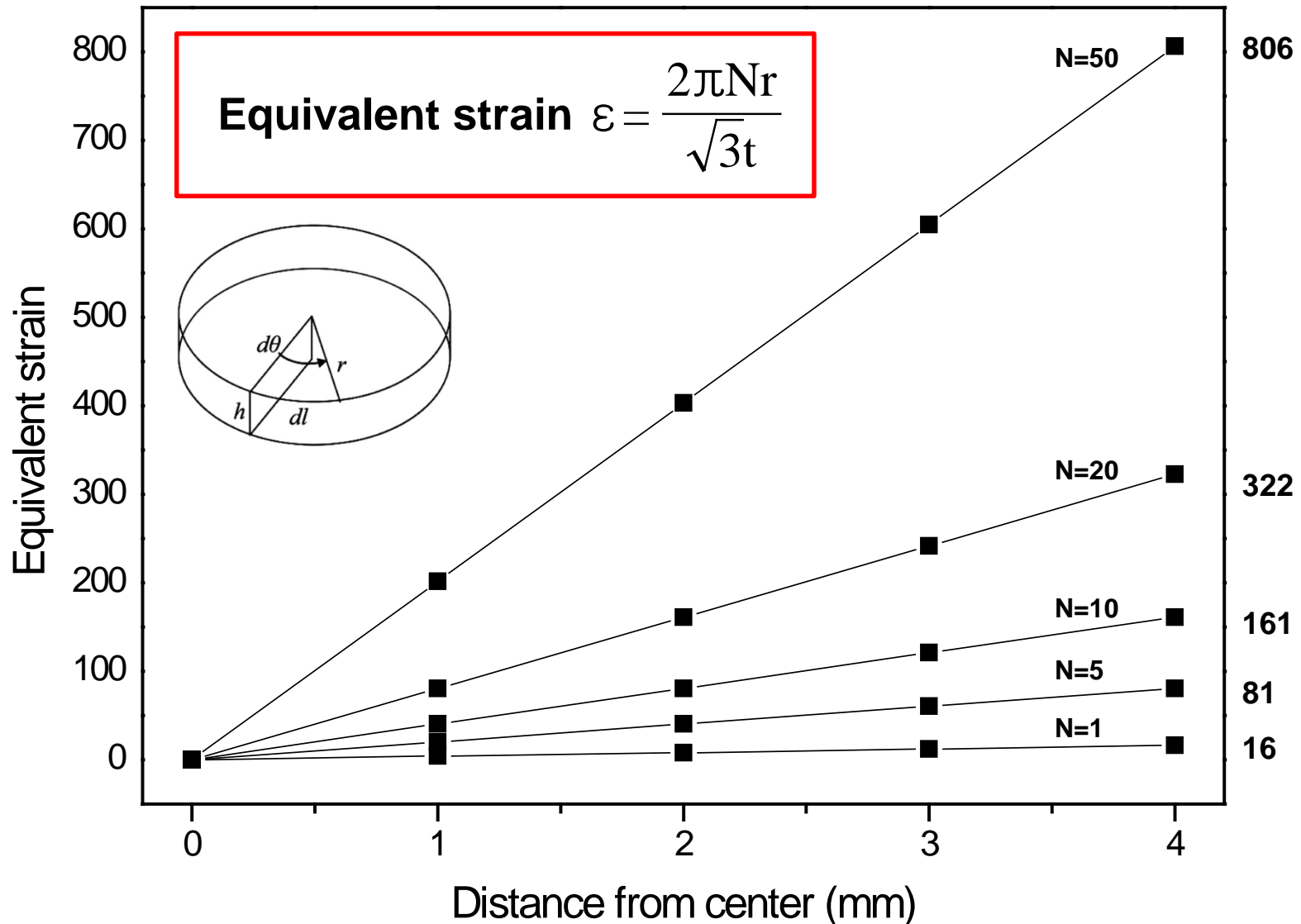
(b)

FIGURE 2.4

equal channel angular extrusion (ECAE)

Schematic diagrams showing the (a) equal channel angular pressing (ECAP) and (b) high-pressure torsion (HPT) processes.

# HPT process: Equivalent strain induced on sample



**HPT: severe plastic deformation, but Inhomogeneous process**

## 2.6.3 Solid-state Processes

### **f. Severe Plastic Deformation : Intense deformation at low temperatures (SPD methods)**

- The SPD methods have some advantages over other methods in synthesizing ultrafine-grained materials. Firstly, ultrafine-grained materials with high-angle grain boundaries could be synthesized. Secondly, the samples are dense and there is no porosity in them since they have not been produced by the consolidation of powders. Thirdly, the grain size is fairly uniform throughout the structure. Lastly, the technique may be applied directly to commercial cast metals.
- However, the limitations of this technique are that the minimum grain size is not very small (typically it is about 200–300nm), and that amorphous phases or other metastable phases have not been synthesized frequently. But, these methods are very useful in producing bulk ultrafine-grained materials.
- The methods of SPD described above have two drawbacks. Firstly, forming machines with large load capacities and expensive dies are required. Secondly, the productivity is relatively low.

## 2.6.3 Solid-state Processes

### g. Accumulative Roll Bonding (ARB process)

: 2 sheets of the same material are stacked, heated (to below the recrystallization temperature), and rolled, bonding the 2 sheets together. This sheet is cut in half, the 2 halves are stacked, and the process is repeated several times. Compared to other SPD processes, ARB has the benefit that it does not require specialized equipment. However, the surfaces to be joined must be well cleaned before rolling to ensure good bonding.

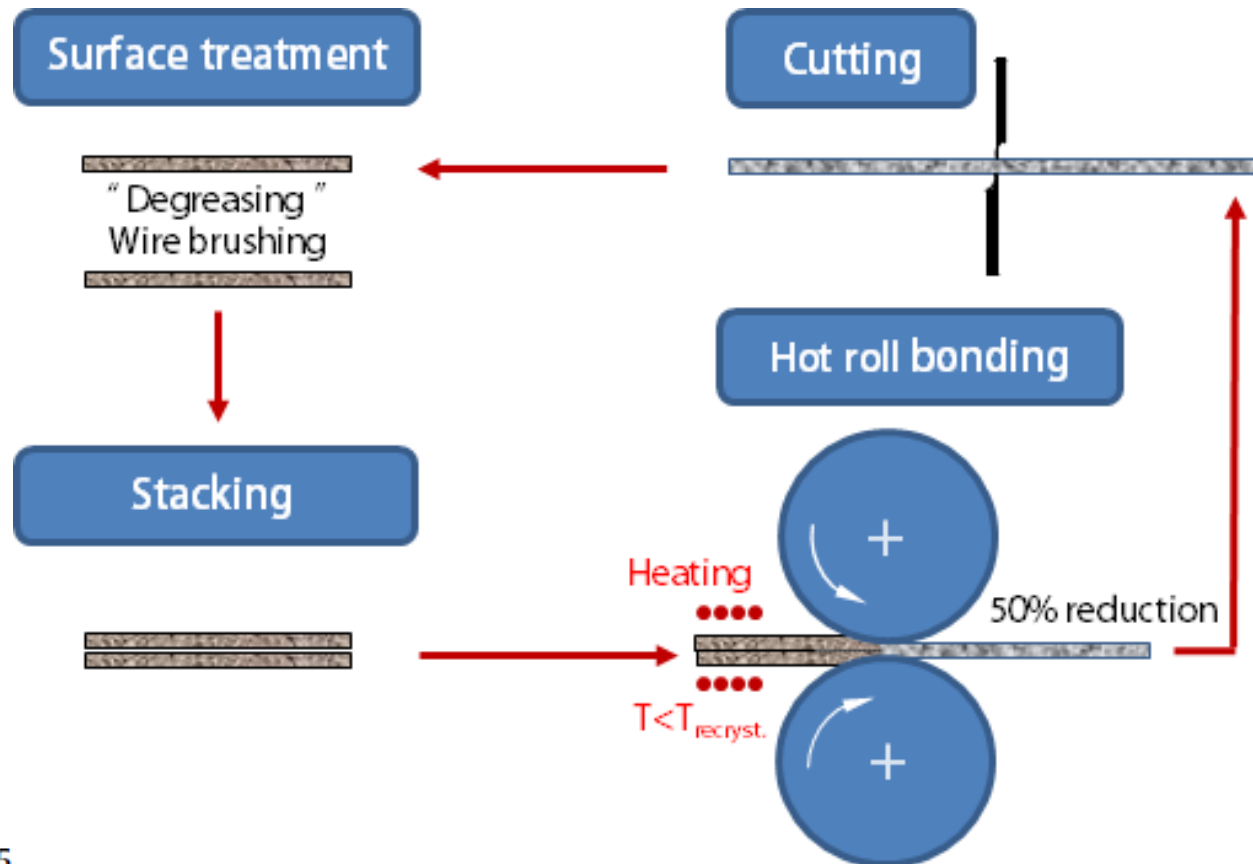


FIGURE 2.5  
Schematic of the accumulative roll-bonding (ARB) process.